IMPROVEMENT OF TEMPORAL RESOLUTION OF FMRI DATA FOR BRAIN DECODING

A THESIS SUBMITTED TO
THE GRADUATE SCHOOL OF NATURAL AND APPLIED SCIENCES
OF
MIDDLE EAST TECHNICAL UNIVERSITY

BY

EMEL VAROL

IN PARTIAL FULFILLMENT OF THE REQUIREMENTS
FOR
THE DEGREE OF MASTER OF SCIENCE
IN
COMPUTER ENGINEERING

FEBRUARY 2022

Approval of the thesis:

IMPROVEMENT OF TEMPORAL RESOLUTION OF FMRI DATA FOR BRAIN DECODING

submitted by **EMEL VAROL** in partial fulfillment of the requirements for the degree of **Master of Science in Computer Engineering Department, Middle East Technical University** by,

Prof. Dr. Halil Kalıpçılar _____
Dean, Graduate School of **Natural and Applied Sciences**

Prof. Dr. Halit Oğuztüzün _____
Head of Department, **Computer Engineering**

Prof. Dr. Fatoş T. Yarman Vural _____
Supervisor, **Computer Engineering Department, METU**

Examining Committee Members:

Assist. Prof. Dr. Hande Alemdar
Computer Engineering Department, METU _____

Prof. Dr. Fatoş T. Yarman Vural
Computer Engineering Department, METU _____

Assist. Prof. Dr. Serdar Çiftçi
Computer Engineering Department, Harran University _____

Date: **10.02.2022**

I hereby declare that all information in this document has been obtained and presented in accordance with academic rules and ethical conduct. I also declare that, as required by these rules and conduct, I have fully cited and referenced all material and results that are not original to this work.

Name, Last Name: EMEL VAROL

Signature :

ABSTRACT

IMPROVEMENT OF TEMPORAL RESOLUTION OF FMRI DATA FOR BRAIN DECODING

Varol, Emel
M.S., Department of Computer Engineering
Supervisor : Prof. Dr. Fatoş T. Yarman Vural

February 2022, 67 pages

In this study, we aim to increase the accuracy of the mapping between the states of the brain and problem-solving phases namely planning and execution. To create a computational model to generate the mapping, an fMRI dataset obtained from subjects solving the Tower of London problem has been used. fMRI data is suitable for this problem as it provides regional and time-varying changes in brain metabolism. However, developing the model using fMRI data is not trivial. Generally, fMRI data has a very large feature vector while having a small sample size due to the scanner limitations. We propose two methods to overcome these limitations and increase the mapping performance. Both methods have a preliminary stage where we perform preprocessing. Preprocessing stage includes feature selection and whitening. The proposed methods are built with polynomial regression and neural networks utilizing the spatial and temporal nature of the data.

Keywords: fMRI, Tower of London, Brain Decoding, Complex Problem Solving

ÖZ

BEYİN ŞİFRESİ ÇÖZÜMÜ İÇİN FMRG VERİSİNİN ZAMANSAL ÇÖZÜNÜRLÜĞÜNÜN GELİŞTİRİLMESİ

Varol, Emel
Yüksek Lisans, Bilgisayar Mühendisliği Bölümü
Tez Yöneticisi : Prof. Dr. Fatoş T. Yarman Vural

Şubat 2022, 67 sayfa

Bu çalışmada, beynin durumları ile problem çözme aşamaları olan planlama ve yürütme arasındaki haritalamanın doğruluğunu artırmayı hedefliyoruz. Haritalamayı oluşturan bir hesaplama modeli oluşturmak için, Londra Kulesi problemini çözen deneklerden elde edilen bir fMRG veri seti kullanılmıştır. fMRG verileri, beyin metabolizmasında bölgesel ve zamana göre değişen değişiklikleri sağladığı için bu problem için uygun bir veridir. Ancak, fMRG verilerini kullanarak model geliştirmek kolay değildir. Genellikle fMRG verileri, tarayıcı sınırlamaları nedeniyle az bir örnek miktarına sahipken çok büyük bir nitelik vektörüne sahiptir. Bu sınırlamaların üstesinden gelmek ve haritalama performansını artırmak için iki yöntem öneriyoruz. Her iki yöntemin de ön işleme yaptığımız bir ön aşaması vardır. Ön işleme aşaması, özellik seçimi ve beyazlatmayı içerir. Önerilen yöntemler, verilerin uzamsal ve zamansal yapısını kullanan polinom regresyon ve sinir ağları ile oluşturulmuştur.

Anahtar Kelimeler: fMRG, Londra Kulesi, Beyin Şifresini Çözme, Karmaşık Problem Çözümü

To all my loved ones

ACKNOWLEDGMENTS

I would like to express my heartfelt appreciation to my beloved Erbil who unconditionally supported me. I would not have completed this thesis without his positivity, help, brilliant suggestions, encouragement, love and comforting.

I owe the biggest thanks to Prof. Dr. Fatoş T. Yarman Vural who patiently helped me through this journey. She has always been there whenever I need motivation and her invaluable guidance. She believed in me and provided constructive feedback.

I want to express my deepest love and gratitude to my family. I am very thankful for my father, Çetin, my mother, Zehra and my dear brother Onur. I am lucky to have their love, encouragement and comforting. They have done everything in their power for me to be successful.

I would like to express my heartfelt thanks to Yakışkan family, Yahya, Şadiye and Onur Yakışkan, who have been a second family to me. They have always loved and supported me. I feel truly blessed to have them by my side.

I would like to thank my friends Merve Taplı, Hüseyin Aydın, Cem Önem, Ezgi Ekiz and Güneş Sucu for their friendship, answering my questions tirelessly and support.

I give thanks to my friends Cansu Alptekin, Pınar Bil, Nazlı Özge Uçan, Zeynep Akkalyoncu, Süleyman Can Özülkü, Melis Ateş and Öykü Koçan who have brought joy to my life.

I want to thank the committee members Assist. Prof. Dr. Hande Alemdar and Assist. Prof. Dr. Serdar Çiftçi for taking the time to review my thesis and their advices.

I acknowledge that this study has been supported by TÜBİTAK (The Scientific and Technological Research Council of Turkey) BİDEB through 2210-A National Scholarship Programme for MSc Students during my M.Sc. education.

TABLE OF CONTENTS

ABSTRACT v

ÖZ vii

ACKNOWLEDGMENTS x

TABLE OF CONTENTS xi

LIST OF TABLES xv

LIST OF FIGURES xvii

LIST OF ABBREVIATIONS xx

CHAPTERS

1 INTRODUCTION 1

1.1 Problem Definition 2

1.2 Proposed Method 3

1.3 Contribution of This Thesis 3

1.4 Outline Of The Thesis 4

2 BACKGROUND FOR BRAIN DECODING PROBLEM BASED ON FMRI DATA 5

2.1 fMRI Background and Characteristics 5

2.2 fMRI Data And Brain Decoding 6

2.3 The Data Set: An fMRI Study of the Tower of London 8

2.4 Structure of fMRI Data 10

2.5 Brief Explanation of Machine Learning Methods For Brain Decoding 11

2.5.1 Voxel Selection 12

2.5.2 Data Augmentation 12

2.5.2.1 Polynomial Regression 13

2.5.2.2 Neural Networks 14

2.5.3 Classification 17

2.5.3.1 Support Vector Machines 17

2.6 Related Work 19

2.7 Chapter Summary 21

3 A NEW SPATIO-TEMPORAL MODEL FOR FMRI DATA AUGMENTATION 23

3.1 A Spatio-Temporal Data Augmentation Method 23

3.1.1 Voxel Selection Using ANOVA 24

3.1.2 Whitening Transformation 25

3.1.3 Interpolation of fMRI Data For Increasing the Time Resolution 26

3.1.3.1 Interpolation By Polynomial Regression 28

3.1.3.2 Interpolation By Neural Networks . . 30

3.1.4 Decoding the Planning and Execution Phases of TOL Game 32

3.2 Chapter Summary 32

4 EXPERIMENTS ON MEASURING THE EFFECT OF INTERPOLATION OF FMRI DATA ON BRAIN DECODING 33

4.1 Software and Hardware Configuration for Brain Decoding Experiments 33

4.2 Experiments On TOL Data Set For Testing And Analyzing the Suggested Data Augmentation Model 34

4.2.1 Analysis of the Interpolated fMRI Data 38

4.2.1.1 Entropy Analysis 43

4.2.1.2 Fourier Transform Plots and Analysis . 51

4.2.1.3 Complexity and Scalability 54

4.3 Chapter Summary 57

5 CONCLUSION 59

5.1 Summary 59

5.2 Discussion 61

5.3 Future Work 61

REFERENCES 63

LIST OF TABLES

TABLES

Table 2.1 Subject details of experiment setup. 9

Table 2.2 The structure of the session data for a participant. 11

Table 4.1 Brain decoding accuracy results for the original fMRI data. 35

Table 4.2 Brain decoding accuracy results for the fMRI data interpolated by the polynomial regression. 36

Table 4.3 Brain decoding accuracy results for the fMRI data interpolated by the proposed neural network method. 37

Table 4.4 Brain decoding accuracy results for the fMRI data interpolated by the proposed neural network method. 37

Table 4.5 Brain decoding accuracy results for the fMRI data interpolated by the simple neural network method illustrated in Figure 4.3. 38

Table 4.6 Region Entropy Estimation (Averaged for all sessions and subjects) (bits/sample). 50

Table 4.7 Region Entropy Estimation for Planning Phase (Averaged for all sessions and subjects) (bits/sample). 50

Table 4.8 Region Entropy Estimation for Execution Phase (Averaged for all sessions and subjects) (bits/sample). 51

Table 4.9 Total time spent on data generation for subject 146 session 3 data. . 56

Table 4.10 Brain decoding performance summary of the proposed method. . . . 57

LIST OF FIGURES

FIGURES

Figure 2.1 fMRI image acquisition summary. 10

Figure 2.2 Biological Neuron. 14

Figure 2.3 Perceptron introduced by Frank Rosenblatt [28]. 15

Figure 2.4 An artificial neural network with one hidden layer. 16

Figure 2.5 An Overview of SVM. 18

Figure 3.1 Pipeline of Procedures. 24

Figure 3.2 Voxel intensity vs. Time plot illustration to explain the labeling of the generated samples. 28

Figure 3.3 Voxel intensity vs. Time plot (Voxel 770, first 3 puzzles from session 3, subject 146). 29

Figure 3.4 Neural network model for interpolation. 31

Figure 4.1 Average number of voxels selected from each anatomical region across all subjects. 34

Figure 4.2 Average Sum of Abs Error of Puzzles In Each Epoch (NN Method - Subject 146, Session 3 with 25k Voxels). 36

Figure 4.3 The simple neural network that is experimented before experimenting our suggested method which is described in Section 3.1.3.2. 38

Figure 4.4 The original voxel intensity values vs. Time plot of voxel with id 770. 39

Figure 4.5 The voxel intensity values vs. Time plot of voxel with id 770 after improving temporal resolution by polynomial regression of degree 6. . . . 40

Figure 4.6 The voxel intensity values vs. Time plot of voxel with id 770 after improving temporal resolution by the method using neural networks. . . . 41

Figure 4.7 The voxel intensity values vs. Time plot of voxel with id 770 after improving temporal resolution by the method using neural networks for the first 3 puzzles only. 41

Figure 4.8 The voxel intensity values vs. Time plot of voxel with id 770 after improving temporal resolution by the method using neural networks for the puzzles with id 10-11-12-13 only. 42

Figure 4.9 Region entropy estimations for samples labeled as planning phase. Averaged for all sessions and subjects, calculated using all data sets: the original fMRI data, the interpolated fMRI data by the polynomial interpolation of degree 6 and the interpolated fMRI data by the proposed neural network method. 45

Figure 4.10 Region entropy estimations for samples labeled as execution phase. Averaged for all sessions and subjects, calculated using all data sets: the original fMRI data, the interpolated fMRI data by the polynomial interpolation of degree 6 and the interpolated fMRI data by the proposed neural network method. 46

Figure 4.11 Region entropy estimations for the session 5 of subject 175, calculated using all data sets: the original fMRI data, the interpolated fMRI data by the polynomial interpolation of degree 6 and the interpolated fMRI data by the proposed neural network method. 47

Figure 4.12 Region entropy estimations averaged for all sessions of subject 146, calculated using all data sets: the original fMRI data, the interpolated fMRI data by the polynomial interpolation of degree 6 and the interpolated fMRI data by the proposed neural network method. 48

Figure 4.13 Region entropy estimations averaged for all sessions and subjects, calculated using all data sets: before interpolation, after polynomial interpolation (degree=6) and after neural network interpolation. 49

Figure 4.14 The Fourier Transform of the original voxel intensity vs. Frequency plot of voxel with id 770. 52

Figure 4.15 The Fourier Transform of voxel intensity vs. Frequency plot of voxel with id 770 after improving temporal resolution by the polynomial interpolation method. 53

Figure 4.16 The Fourier Transform of voxel intensity vs. Frequency plot of voxel with id 770 after improving temporal resolution by the neural network method. 54

LIST OF ABBREVIATIONS

MVPA	Multi-voxel Pattern Analysis
MRI	Magnetic Resonance Imaging
fMRI	functional Magnetic Resonance Imaging
BOLD	Blood Oxygen Level Dependent
SVM	Support Vector Machine
ReLU	Rectified Linear Unit
GAN	Generative Adversarial Network
TOL	Tower of London
PR	Polynomial Regression
AAL	Automatic Anatomical Labeling

CHAPTER 1

INTRODUCTION

Have you ever wondered what happens in your brain when you are solving a puzzle or any kind of problem? As humans, we live in a chaotic world with a wide range of problems to solve everyday. We constantly think and design solutions for problems to survive or to have fun. Human brain is the creator of most of the problems and solutions to them. Besides being a designer, human brain is the one making us able to produce relevant moves for these solutions. The set of type and factor variations for the problems we encounter throughout our lives have an unimaginable size. Therefore, human brain, which is the commander that makes us survive in the middle of this world of problems, is a mysterious organ for the researchers.

With the advances in the technology, activation in the brain can be visualized now. Pictures of the brain can be taken while complex problems are being solved which gives researchers opportunity to analyze this mysterious organ. There are many different brain imaging techniques to monitor the functioning of human brain. Electroencephalography (EEG) measures the electrical activity in the brain while Positron Emission Tomography (PET) reveals the metabolic or biochemical function of the brain using a radioactive tracer. Magnetic Resonance Imaging (MRI) and functional Magnetic Resonance Imaging (fMRI) measure the changes in Blood Oxygen Level (BOLD) signals. Functional Magnetic Resonance Imaging (fMRI) is the most popular technique to conduct experiments for analyzing how human brain works and understanding functioning of the human brain.

1.1 Problem Definition

fMRI is widely used in brain decoding, which is finding the relations between the patterns of neural activation and the performed tasks, for complex problem solving. We predict the cognitive state of a subject at a given time instance by analyzing the brain image (fMRI) captured at that moment. Generally, fMRI data have a high spatial resolution meaning that they have a very large feature vector compared to Electroencephalography (EEG), Functional near-infrared spectroscopy (FNIRS) and other brain data. Due to scanner limitations, retrieving high resolution images decreases the sample acquisition rate. A small number of brain volumes can be captured as a result of the limitations. High spatial and low temporal resolution of the data arises a problem called the Curse of Dimensionality when estimating the parameters of the classifier for brain decoding. Bellman [4] defines the Curse of Dimensionality saying that the number of samples required to estimate an arbitrary function grows exponentially with the number of input variables for a given level of accuracy. The Curse of Dimensionality problem reduces the generalization and the classification performance of the classifier that is used for cognitive state decoding. In this thesis, the goal is to increase the cognitive state classification performance by increasing temporal resolution of the fMRI data.

In this thesis, Tower of London (TOL) data set, which consists of fMRI images collected while subjects were solving a computerized version of the TOL, is used to develop the solution for the described problem. The data set has around 600 brain volumes per session while it has a feature vector of size 185405. The data set has also sparsity problem as many of the features do not contribute to cognitive task. We do not have sufficient number of samples to estimate a brain decoding model for a feature vector of this size. In other words, the nature of the data set makes it almost impossible to optimize a classifier properly.

1.2 Proposed Method

In this study, we propose a computational model for temporal interpolation of fMRI data. The main focus of this thesis is to overcome the Curse of Dimensionality and sparsity problem in the fMRI data. In order to decrease the effects of Curse of Dimensionality problem, reducing the feature space or generating synthetic samples using machine learning methods are the first solutions that comes to mind but they also have some drawbacks.

Reducing feature space is one of the ways to overcome the Curse of Dimensionality and sparsity but it leads to information loss and decrease in classification performance. Sample generation is another solution but it requires a huge computation power considering the feature space in TOL data set. Although these solutions are not enough or feasible alone, proposing a combination of them would be an intelligent way to solve the problems due to the nature of fMRI data. In order to experiment and verify this, we are going to design an interpolation method to generate samples after selecting a method for feature selection.

Our method consists of feature selection, data augmentation and normalization. Following that, a classifier is estimated to create a mapping between human brain activity and complex problem solving stages.

1.3 Contribution of This Thesis

Preprocessing of the fMRI data is essential to achieve a high performance on the classification of fMRI images according to complex problem solving stages. As many previous studies also propose, feature selection, temporal interpolation and of course normalization need to be performed in preprocessing stage. This study proposes two novel methods for temporal interpolation on top of voxel selection using ANOVA and normalization.

In Section 2.6, we overview the related work on data augmentation methods. It is

mentioned that generative neural networks are widely used for data augmentation. Cubic spline interpolation and support vector regression are also used for generation of complementary data. In this study, first a polynomial regression model is introduced as a interpolation method. As the second proposed model, a complex neural network is trained to generate samples. Polynomial regression estimates a simple function for voxel intensities at a given time. This is a method that was inspired by voxel instensity-time plots since a signal for a given voxel looks very similar to a polynomial function. Regression was used for fMRI sample generation in the previous works [36]. However, only the polynomial regression was not considered in these applications. The proposed neural networks model the data set as a nonlinear function with multiple parameters utilising time and voxel coordinate information. Because of the nonlinear behavior of fMRI signals, a higher order nonlinear function is needed to model intensities. Unlike the GAN method mentioned in Section 2.6, this is a fully connected architecture and unlike cubic spline interpolation, the methods proposed make use of the temporal and spatial nature of the data set. Besides, these models estimate nonlinear functions with high degrees avoiding underfitting.

1.4 Outline Of The Thesis

In Chapter 2, we present the background information on this thesis. Brain decoding, fMRI, the Tower of London data set and machine learning methods are overviewed.

Chapter 3 introduces our method to increase the temporal resolution of fMRI data. This chapter explains the steps of the proposed method which consists of feature selection, data augmentation, normalization and brain decoding.

Chapter 4 presents the brain decoding performances after temporal interpolation. In addition, the results are discussed by comparing the classification results, providing Fourier Analysis and Shannon Entropy calculations.

In Chapter 5, the overall outcomes of this study are summarised and discussed. Then, the possible directions of this thesis are briefly described.

CHAPTER 2

BACKGROUND FOR BRAIN DECODING PROBLEM BASED ON FMRI DATA

In this chapter, the aim is to give an overview to functional magnetic resonance imaging (fMRI) studies, the characteristics of fMRI imagery and bring an understanding of brain decoding. The Tower of London data set (TOL), which the proposed models are implemented on is introduced and explained. Then, the required domain knowledge to understand this study, on machine learning methods is provided. In addition, the data generation and interpolation methods are surveyed while focusing separately on general approaches and the methods used in fMRI studies.

2.1 fMRI Background and Characteristics

Medical imaging technology has reached to an era in which it is possible to retrieve scans of our bodies and create three dimensional models of organs to be able to analyze abnormalities and detect diseases. [33] Blood Oxygen Level Dependent (BOLD) functional magnetic resonance imaging (fMRI) is one of the technologies to capture the activities in our brain in four dimensional space-time images. Besides diagnosis, it helps us to relate what we do or think with blood oxygen levels in different regions of our brain. fMRI data enable us to understand what happens in our brains and decode our mental states.

The discovery of fMRI dates back to 1936 by Pauling and Coryell and the use of it continuously increasing in neuroscience studies. fMRI is extensively used in neuro-

science research because it can be performed on a clinical 1.5T scanner, relatively low cost and high spatial resolution. [9]

fMRI helps us to detect regional and time varying changes in the brain metabolism. The changes in the metabolic state of the brain is measured by MRI machine through the scan. Detectable effects can be observed as a result of the changes in the oxygenation level of hemoglobin which create fluctuations in the local MR signal known as the blood oxygenation dependent (BOLD) effect. [34]

In fMRI experiments, subjects are asked to perform a simulation which is a combination of a series of cognitive tasks. Subjects are asked to do specific tasks such as playing a game, solving a mathematical problem, listening to a music or gambling while fMRI data is collected. In this study, the complex problem solving phases namely the resting, planning and execution states of the obtained scans are considered. The data consists of the time series for each unit volume of the brain, which can be used to examine correlation between signal values and stimulus. The collected images show which anatomic region of the brain is active at a given time. Oxygen consumption increases in the anatomic regions of the brain which are relevant to the performed task, as a result of the activation of the responsible neurons.

Voxel is the building block of fMRI images with a volume about $1mm^3$ containing 4-5 thousands of neurons. fMRI images have high dimensionality which can vary according to the characteristics of fMRI machine. Each scan used in this study contains around 180000 voxels. Also, a scan with that much resolution takes a noticeable amount of time and the retrieved data is not continuous. Therefore, the number of scan samples is very small compared to the resolution of the scans.

2.2 fMRI Data And Brain Decoding

Brain decoding aims to find the relations between the patterns of neural activation in the human brain and the tasks performed during the retrieval of brain scans. Multi Voxel Pattern Analysis (MVPA) can be used in brain decoding. MVPA is employed to recognize cognitive states by voxel signal values using machine learning meth-

ods. Principal component analysis, voxel selection methods, data generation, support vector machines and neural networks are widely used MVPA methods. [14, 23]

Before classification methods are utilized to detect relations between scans and the tasks, voxel selection or data generation is required to overcome the Curse of Dimensionality. In most neuroimaging studies, the sample size is too small compared to voxel number in an image. Temporal resolution is low for the images with the huge number of non-zero voxels due to the sampling frequency because of the MR machine limitations. For the high resolution scans with more than 100000 voxels, the sample size generally is lower than 1000. Therefore the number of features outnumber the sample size, which is known as curse of dimensionality, in many studies. [19, 5] The Tower of London data set, which will be introduced in detail, is used in the implementation of the proposed methods. Curse of dimensionality is a challenge we face in TOL data set as well. Number of voxels in each sample is around 180 000 but we only have 590 time instances per session.

Voxel selection, which reduces the number of voxels, is a popular way of overcoming the Curse of Dimensionality problem in the fMRI studies. Besides reducing the effect of the Curse of Dimensionality in brain decoding performance, voxel selection is utilised to avoid overfitting and improve classification accuracy. Most of the time, the limitation on the computational resources is another problem while working with a brain volume with high number of voxels. Feature reduction methods are helpful as it reduces the computational resources needed for the brain decoding experiments. There are many popular feature reduction methods. Principal component analysis and independent component analysis are commonly used unsupervised feature reduction methods. ANOVA and Pearson Correlation Coefficient approaches are some of the supervised feature reduction methods used in fMRI studies. [19]

Some studies select specific brain regions which are related to a prescribed cognitive task to reduce the dimensionality. Also, averaging voxel intensities over each anatomical region (AAL) is possible for reducing the dimension of fMRI voxel features. [6] proposes a method to cluster voxels into spatially coherent regions of homogeneous functional connectivity. Generated clusters can be utilised in feature reduction simi-

larly.

In addition to feature reduction by selecting the informative voxels at each anatomic region or averaging the voxel time series, data augmentation is also an approach to overcome the Curse of Dimensionality problem. Instead of reducing feature space size, the sample number can be increased by data augmentation. Interpolation and regression methods can be utilized to place extra scans between the original scans acquired.

There are a wide range of methods to define a feature space based on fMRI data. In this study, the feature space is voxel intensity values at a particular time instance. The cognitive task which is performed at that particular time defines the label. Following the mentioned methods to overcome curse of dimensionality and improve generalization of the data, fMRI scans are classified into tasks using mostly nonlinear supervised machine learning methods such as SVM and neural networks.

2.3 The Data Set: An fMRI Study of the Tower of London

Complex problem solving has been a popular topic in Neuroscience for decades due to its importance in high-level tasks. Planning and executing a task are crucial parts of human life. The underlying cognitive processes or the neural architecture behind problem solving has not been uncovered completely yet. Tower Of London (TOL) task developed by Shallice (1982) is one of the tasks that has been extensively used to evaluate complex problem solving and planning function. [22] The setup of Tower of London task is composed of 3 bins with different capacities and 3 balls with different colors located on the bins. The task it to reorganize the balls from the initial state to a goal state while moving one ball at a time in the minimum number of moves. [2] Some of the studies conducted on the TOL task have shown that especially frontal lobe syndrome patients performed poorly on the TOL. As an implication of that, the findings have been accepted as a proof that the frontal cortex has a connection with planning processes. [31, 22] TOL is a popular task to examine a variety of clinical disorders including Parkinson's [17], Huntington's [15] and autism [11]. The task

has recently been employed by the investigators to examine complex problem solving processes of normal human populations with the help of neuroimaging. [20]

18 participants whose ages ranged between 19 and 38 participated in the computerized version of TOL experiment. Figure 2.1 summarizes this process. They were shown two configurations for each puzzle namely the start and goal state. Balls were moved by clicking on them and clicking on the intended destination bin. Participants were asked to manipulate the start state into goal state using minimum number of moves and they were not informed about the number. Bins presented had different depths and only the top-most ball could be moved. [21] Subjects experienced a practice session and a scanning session. Participants were familiarized with TOL task in practice session. After that, each participant underwent scanning session which includes 4 runs containing 18 different puzzles. Each puzzle had a time limit of 15 second of which the first five seconds were allocated for planning only. Planning time slot could be extended if the participant wanted to continue planning. There was a 12-second resting time between puzzles in which participants focused on a plus sign located on the center of the screen.

Table 2.1: Subject details of experiment setup.

# of subjects	ages	# of sessions per subject	# of puzzles per session
18	19-38	4	18

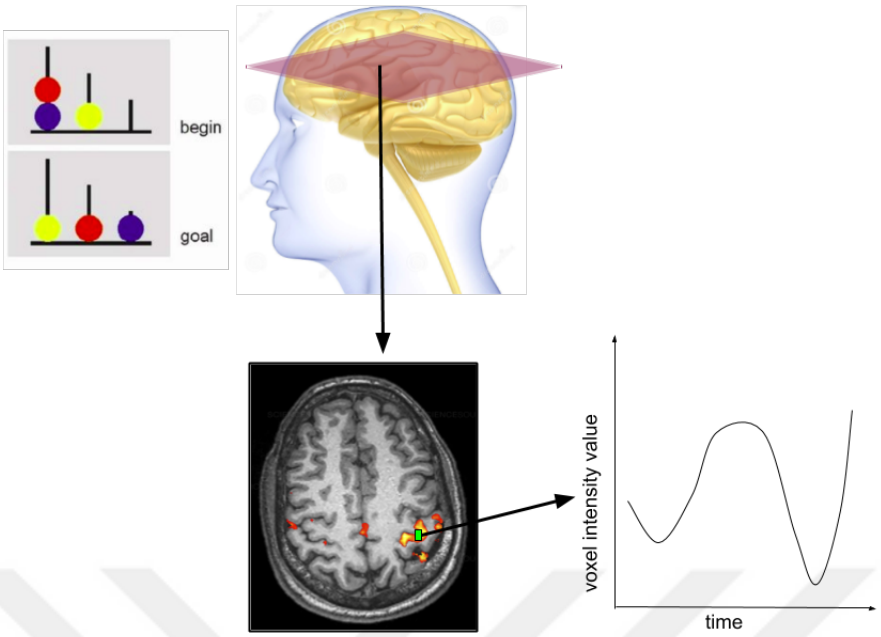


Figure 2.1: fMRI image acquisition summary.

fMRI images were collected using a 3T Siemens TRIO scanner with an 8-channel radio frequency coil located in the Imaging Research Facility at Indiana University. The images were acquired in 18 5 mm thick oblique axial slices using the following set of parameters: TR=1000 ms, TE=25 ms, flip angle=60, voxel size=3.125 mm3.125 mm5 mm with a 1 mm gap [21].

2.4 Structure of fMRI Data

The fMRI data acquired from TOL experiments carries a variety of information including voxel intensity values, voxel coordinates, anatomic region ID's and the label of the cognitive task at each scan, namely planning, execution or resting.

Table 2.2: The structure of the session data for a participant.

attribute	dimensions	details
voxel intensity	(185405, 590)	185405 voxel intensity values (feature vector size/image resoluton) per time sample, 590 time instance (number of samples)
coordinates	(185405, 3)	(x,y,z) coordinate values of each voxel in brain images
regionIDs	(185405,1)	anatomical region id for each voxel in brain images

In this thesis, the time series input vector for the i^{th} voxel for a session with T time instances is referred as V_i:

$$V_i = [V_i(1), V_i(2), V_i(3), \ldots, V_i(T-1), V_i(T)], \tag{2.1}$$

and spatial index of i^{th} voxel is (x_i, y_i, z_i).

Let the number of voxels in a sample be n. Spatial input vector for a brain volume at time t is named as $S(t)$:

$$S(t) = [V_1(t), V_2(t), V_3(t), \ldots, V_{n-1}(t), V_n(t)] \tag{2.2}$$

And label of the cognitive state at time t is defined as:

$$y(t) \in [execution, planning] \tag{2.3}$$

2.5 Brief Explanation of Machine Learning Methods For Brain Decoding

In this section, background information needed for essential steps of the models proposed will be introduced. There will be three main topics, namely, voxel selection, data augmentation and classification.

2.5.1 Voxel Selection

In this thesis, an Analysis of Variance (ANOVA) feature selection method is used to reduce the number of features in $S(t)$ defined in Equation 2.3. Voxel selection selects the voxels which contribute to the cognitive process and discard the remaining ones. Also, ANOVA voxel selection makes the space and time complexity of the analysis on the data set feasible given the large number of voxels in each brain volume.

We calculate f-value scores for each voxel. The voxels are ordered according to their f-value scores and the most discriminative voxels in terms of f-value score are selected.

f-value score for a given voxel V_i with label vector y_i is calculated as:

$$f_i = \frac{MSB(V_i, y_i)}{MSW(V_i, y_i)} \tag{2.4}$$

where y_i is the label that indicates the subtask namely planning or execution. $MSB(V_i, y_i)$ is the mean square value between V_i and y_i as shown in equation 2.5,

$$MSB(V_i, y_i) = \frac{SSB(V_i, y_i)}{df_{between}}, \tag{2.5}$$

$SSB(V_i, y_i)$ is the sum of squares between V_i and y_i and $df_{between}$ is number of qroups (planning and execution) minus one.

$MSW(V_i, y_i)$ is the mean square value within V_i and y_i. It can be formulated as shown in equation 2.6

$$MSW(V_i, y_i) = \frac{SSW(V_i, y_i)}{df_{within}} \tag{2.6}$$

where $SSW(V_i, y_i)$ is the sum of squares within group and df_{within} is the total number of elements in V_i minus number of groups, which is called as the degree of freedom.

2.5.2 Data Augmentation

Data augmentation in the context of this thesis is that estimating a continuous function to model voxel intensity time series to generate intensity values at the missing time

instances. fMRI data has a high dimensional feature space, which means a high number of voxels in each brain volume, while it has small number of samples due to scanner limitations. This leads to poor generalization performance on the classifier used in brain decoding. Data augmentation is used to generate fMRI scans to increase the generalization and brain decoding performance.

In this thesis, neural networks and polynomial regression are used in temporal interpolation of fMRI data. This chapter gives the background information on these methods.

2.5.2.1 Polynomial Regression

In this study, as a baseline we use polynomial regression to insert time samples. Polynomial regression is a method of regression analysis in which $V_i(t)$ is estimated as an k^{th} degree polynomial of the independent variable t. It is utilized to find a nonlinear relationship between the time t and the corresponding voxel intensity $V_i(t)$.

The purpose of the regression analysis is to compute the expected value of $V_i(t)$ in terms of t where $V_i(t)$, $t \in R$. The simple linear regression model is:

$$V_i(t) = \beta_0 + \beta_1 t + \epsilon_i \tag{2.7}$$

where ϵ_i is a random error with zero mean. This linear relationship may not be enough to model nonlinear relations as it will most likely underfit.

Polynomial regression can be employed to model data sets that can be visualized as curves. The polynomial function of order k can be defined for voxel intensity time series as,

$$V_i(t) = \beta_0 + \beta_1 t + \beta_2 t^2 + \beta_3 t^3 + ... + \beta_k t^k + \epsilon_i, \tag{2.8}$$

2.5.2.2 Neural Networks

Considering the fact that fMRI voxel time series are nonlinear functions of time, in this study, neural networks are employed to interpolate the voxel time series $V_i(t)$ using regression. Therefore, it is needed to have an understanding about how neural networks can be used as a nonlinear function interpolator.

Our brains process information using a network of neurons. Neurons receive an input and process it. Then, they deliver the output of electric signals to the neurons they are connected to. Artificial neural networks works roughly with the same principle. Figure 2.2 and 2.3 exhibit the similarity between a biological neuron and an aritificial neuron.

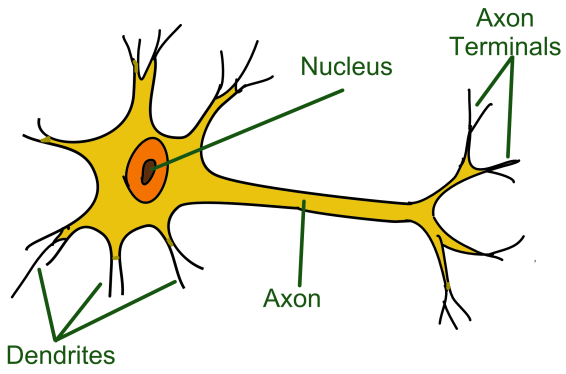


Figure 2.2: Biological Neuron.

A neural network is a machine learning model inspired by the human brain, which are designed to recognize patterns. Artificial neural networks share the same structure with natural networks of neurons, which gives them much more prediction performance over the previously used regression models.

Perceptron can be thought as a basic artificial neuron. It takes several inputs and the computes the weighted sum of them. It applies an activation function on the weighted sum. If the weighted sum is bigger than a threshold, it returns 1 otherwise it returns 0. A perceptron can only be used for implementation of linearly separable functions.

To model nonlinear functions, a network of neurons is necessary.

The perceptron introduced by Frank Rosenblatt [28]. Perceptron is an algorithm for learning a binary classifier that maps real valued input vector v to an output of $f(v)$ such that,

$$f(v) = \begin{cases} 1 & w \cdot v + b \geq 0 \\ 0 & otherwise \end{cases} \tag{2.9}$$

where w is a vector of weights with real values, $w \cdot v$ is the dot product $\sum_{i=1}^{n} w_i v_i$, n is the number of inputs to the Perceptron and b is the bias. Figure 2.3 illustrates the Perceptron algorithm as formulated in Equation 2.9.

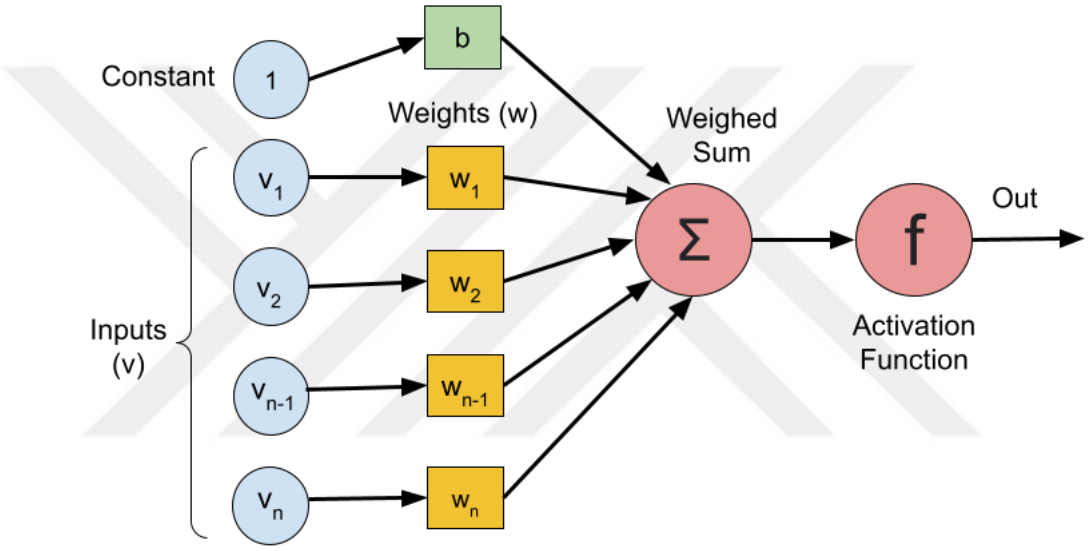


Figure 2.3: Perceptron introduced by Frank Rosenblatt [28].

Loosely speaking, neural networks are multi-layer Perceptron units that are organised in a hierarchy for various machine learning tasks, such as, clustering, classification and regression. It accepts a set of observations to estimate the network parameters to be able to predict the nature of an unknown sample.

A neural network is composed of three main layers as illustrated in Figure 2.4. Input layer is the layer that inputs the data to be processed by the network. Each neuron in this layer takes one feature of the input. Hidden layers do all of the processing job in the network. A neural network can have one or more hidden layer. In hidden layers,

neurons receive the outputs of the neurons in the previous layer as their input. After that, they multiply the input by weight and add the bias. Output layer assemble the output from the last hidden layer and output it after applying an activation function.

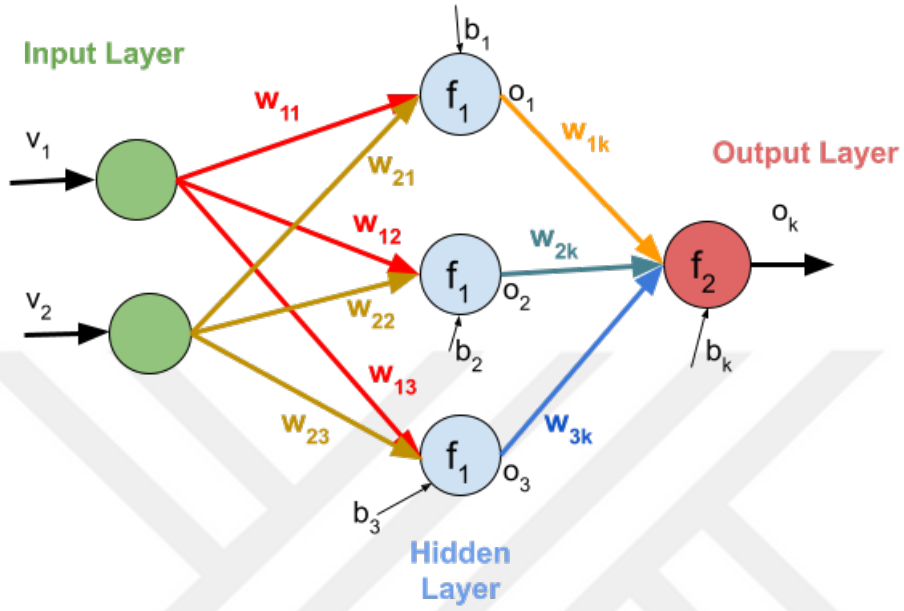


Figure 2.4: An artificial neural network with one hidden layer.

Figure 2.4 exhibits an example of a fully connected neural network. It takes an input vector with 2 features, namely, v_1 and v_2.

Equation 2.10 formulates the output o_j from the hidden layer. w_{ij} corresponds to weights and b_j is the bias for the hidden layer. f_1 is the activation function used in this layer:

$$o_j = f_1(\sum_{i=1}^{2} w_{ij} v_i + b_j), \text{ where } j \in [1, 2, 3] \tag{2.10}$$

Equation 2.11 formulates the output layer of the neural network. w_{jk} represents the weights and b_k is the bias of the output layer. f_2 is the activation function applied to the weighed sum in the output layer. o_k corresponds to the output of the neural network.

$$o_k = f_2(\sum_{j=1}^{3} w_{jk} o_j + b_k) \tag{2.11}$$

Training process of a neural network is a procedure to find optimal weights and biases that minimizes the error between the network's prediction and the desired result with respect to a cost function. A cost function is a function that determines how well a machine learning model performs for a given set of data. Cost functions calculate the difference between anticipated and expected outcomes and shows it as a single real number. One of the most used cost functions is the sum of the square errors. Backpropagation is the procedure to minimize the cost function.

2.5.3 Classification

2.5.3.1 Support Vector Machines

Support Vector Machine (SVM) introduced by Vapnik [35] is a kernel method for classification of data by mapping it from a nonlinearly separable space to a linearly separable space. Support Vector Machines (SVM) are widely used for classification of fMRI data which requires a nonlinear model.

Kernel functions are used to accomplish the mapping process. After applying kernel functions, the linear separation of data can be performed in the kernel space. This procedure is illustrated in Figure 2.5, in which a kernel function ϕ is used for the mapping.

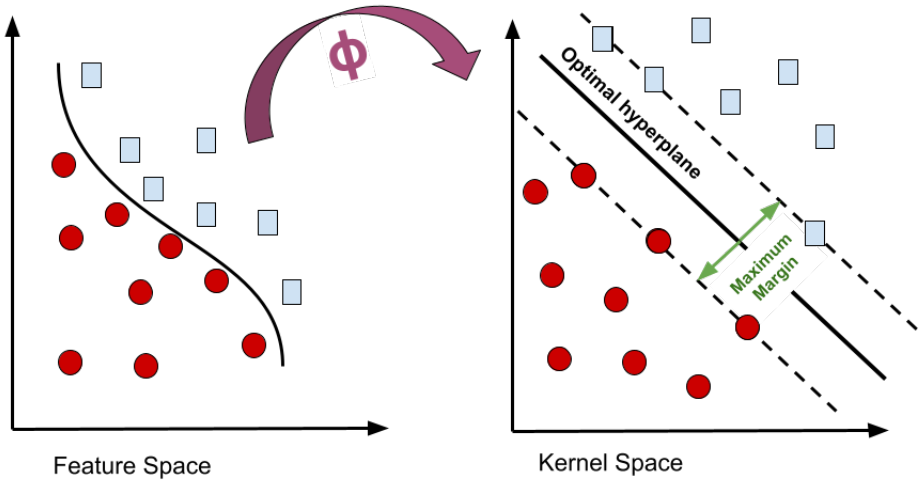


Figure 2.5: An Overview of SVM.

Polynomial and Radial Basis Function (RBF) kernels are widely used for this purpose. RBF kernel is defined as,

$$K_{RBF}(S(t_1), S(t_2)) = e^{-\gamma \|S(t_1) - S(t_2)\|^2}, \tag{2.12}$$

where γ is a parameter which is bigger than zero and it sets the spread of the kernel. $S(t_1)$ and $S(t_2)$ correspond to two brain volumes at time t_1 and t_2

After the kernel function maps the lower dimensional feature space to a higher dimensional kernel space, SVM sets up a hyper plane. The hyper plane that has the largest distance to the closest training sample points (support vectors) of any class (margin) reaches the optimal separation by reducing the generalization error.

In SVM, the aim is to maximize the margin between support vectors and hyper-plane. The loss function to maximize margin is hinge loss in SVM. Hinge loss $L(S(t))$ is formulated as,

$$L(S(t)) = \max\Big(0, 1 - y(t) f(S(t))\Big), \tag{2.13}$$

where $S(t)$ is the input, a brain volume at time t, and $f(S(t))$ is the predicted cognitive state by the SVM for the given input $S(t)$. $y(t)$ is the expected label, cognitive state, of the brain volume $S(t)$ at time t.

The cost is 0 when the label is predicted correctly otherwise the cost is computed as $1 - y(t)f(S(t))$. Regularization parameter can be added to the cost function in order to balance the margin maximization and loss.

After calculating the partial derivatives with respect to the weights which gives the gradients, the weights can be updated. [27]

2.6 Related Work

fMRI data has always been a popular non-invasive technique to record brain activation during a mental process for brain studies. There are studies focusing on complex problem solving using TOL data. Some of these studies also experimented feature reduction and interpolation of the fMRI data.

One of the studies on complex problem solving using TOL data set [1] utilizes voxel selection and interpolation in data processing part of the pipeline proposed to explore the cognitive network dynamics among planning and execution phases of complex problem solving. Voxel selection step is introduced to overcome the Curse of Dimensionality problem. The large number of voxels in each brain volume (185,405 voxels per time instant) is reduced to a set of selected voxels and the noise that is inherent in data is decreased as a result of that. Temporal interpolation to increase the number of brain volumes for each puzzle was needed because of the small sampling rate (1 sample per second) and the short duration of each puzzle (max 15 seconds). ANOVA feature selection is utilised to select the most discriminative subset of voxels which is the new feature set successfully making the space and time complexity of the analysis on data set feasible. After voxel selection, cubic spline interpolation function is used to increase temporal resolution. This method prevents edge effects and smooths the spikes out differently from linear interpolation methods. Data processing is followed by building functional brain networks. The results from each step are classified by

SVM to compare the effect of data processing and generated brain network. The relevant SVM classification results are reported as 74% after 10000 voxels are selected, 81% after interpolation while raw data is giving 60% classification success. This study clearly shows the positive effect of voxel selection and interpolation for sample generation.

[2] describes the same data processing procedures with [1]. It focuses on the steps before building functional brain networks and investigates the effect of interpolation, voxel selection, noise and combination of these methods on classification performance. Voxel selection selects 25000 voxels while the number of selected voxels is 10000 [1].

[36] makes nonlinear estimation and modelling of fMRI data proposing a spatio-temporal support vector regression [35] method for data augmentation. This study introduces a 4D data representation as the feature vector to perform SVR on. fMRI data is spatially divided into small windows, such as 3x3x3 voxel regions. Entire time series for the voxels falling into the small region is taken. Sample generation is done within the respective window using Support Vector Regression (SVR). The intensity time series generated for voxels in spatially overlapped windows are averaged to compensate for the spatial correlation between neighbouring windows. For a given voxel with coordinates (u,v,z) and time point t, feature vector is defined as $\bar{x} = [u, v, z, t]^T$ ($u \in \mathbb{R}$, $v \in \mathbb{R}$, $z \in \mathbb{R}$, $t \in \mathbb{R}$). Full fMRI image size is $S = S_u \times S_v \times S_z$ and S_t is total number of time points. Within each region, number of samples is M where $M = M_u \times M_v \times M_z$. Input samples are $\bar{x} = \bar{x}_1, \bar{x}_2, \bar{x}_3, ..., \bar{x}_M$ and corresponding scalar output intensities are $\bar{y} = \bar{y}_1, \bar{y}_2, \bar{y}_3, ..., \bar{y}_M$. The proposed model is $f_{SVR}([u, v, z, t]^T) = y$. After estimating this model, intensities for new time points can be estimated for voxels and data can be generated. This study presents SVR as a data augmentation method for fMRI data for the first time and it makes use of both coordinate and time information of the voxels. This is a novel method that gives another aspect for fMRI data augmentation.

There are studies on sample generation for fMRI data which utilise generative adversarial networks (GAN) as well. [38] proposes a generative adversarial network to

perform data augmentation on fMRI data. This approach is not suitable for our study since we aim to make use of time information and develop a model for temporal interpolation. GAN architectures do not depend on time instead synthetic samples are generated and discriminator component is tried to be tricked by the generated samples. Besides this, considering GAN to generate more samples brings us back to our main problem, the curse of dimensionality. TOL data set is too small to train a good GAN architecture.

2.7 Chapter Summary

In this chapter, fMRI and brain decoding, TOL data set and the representation of the data are briefly explained. After that, we explain the machine learning methods that are used in the proposed method and related works that are previously done.

CHAPTER 3

A NEW SPATIO-TEMPORAL MODEL FOR FMRI DATA AUGMENTATION

This chapter introduces our proposed methods for temporal augmentation of fMRI data. The main goal is to find a model to generate new data using the information in the observed data and improve the generalization performance of the classifier by training with more samples.

The application of interpolation methods and generative models are surveyed to design the proposed methods. Bi-cubic spline interpolation [13], GAN [38] and SVR [36] are used to increase temporal resolution of fMRI data in the previous studies. SVR, Neural Networks and Polynomial Regression methods are brought together to introduce novel methods for interpolation of fMRI data. To assess the effect of data generation on brain decoding performance, SVM [18], logistic regression [29], neural networks [13] and Gaussian Naive Bayes [8] classifiers are used in the previous studies.

3.1 A Spatio-Temporal Data Augmentation Method

fMRI data is known to have a high spatial resolution and low time resolution compared to the other brain data acqusition data, such as, EEG and FNIRS.

In a typical event based cognitive task experiment, there are total of approximately 200,000 voxels at each brain volume for a given time instance. An fMRI session consists of several dozens of time samples to characterize a cognitive process. If we assume that we represent each brain volume as a labeled feature, the data set consists

of 200,000 dimensional feature vectors for each labeled time samples. Thus, we characterize the data set of couple of dozens of sample in 200,000 dimensional vector space. This problem, called the Curse of Dimensionality, can be attacked by reducing the space dimension and increasing the time samples.

The suggested method consists of 4 stages as illustrated in Figure 3.1:

- Voxel selection to reduce spatial dimension.
- Data generation to increase temporal resolution: Fit voxel intensity time series to a continuous function and recover the intensity values for the missing time instances.
- Perform whitening transformation to normalize the data.
- Classification to evaluate brain decoding performance: Classifier to decode brain volumes to complex problem solving phases.

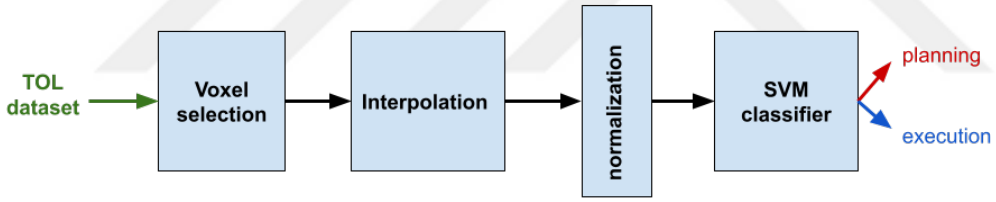


Figure 3.1: Pipeline of Procedures.

3.1.1 Voxel Selection Using ANOVA

As mentioned in the Chapter 2, fMRI data generates voxel intensity values proportional to the neural network activities in each voxel.

If a particular voxel time series is relatively low intensity values, the corresponding voxel location is inactive which means that the particular voxel does not contribute to

the underlying cognitive process. Thus eliminating the inactive voxels not only reduce the dimension but also, removes the noise, contributed by the irrelevant voxels.

Therefore, a voxel selection method should be used before applying designed algorithm to data. Feature reduction methods select relevant voxels for the decoding of fMRI activity patterns. [37] As a result of feature reduction procedure, the most discriminative voxels are used for developing the proposed interpolation methods.

ANOVA is utilized to select the most informative voxels in the TOL data. To use [2] as a baseline for the performance of this study, the total of 185,405 voxels are reduced to 25000 voxels. These are supposed to be the most informative 25000 voxels with respect to the f-value score. Also, 6000 voxels are selected to create a smaller data set for the experiments.

The f-value scores for each voxels are calculated as described in Section 2.5.1. We order the voxels according to their f-value scores. Then, we select 6000 and 25000 voxels with the highest f-value scores to reduce the brain volume and remove redundant voxels.

3.1.2 Whitening Transformation

The noise embedded in the fMRI data may have temporal correlations or noise coloration with the brain activities because of physiological and physical effects outside the brain. [25] The temporal correlation is a result of neural and hemodynamic sources, scanner-induced low-frequency drifts and cardiac pulsation. [24] Temporal correlation present in the noise signal of fMRI data complicates the estimation of active brain regions resulted by an external stimulus. This might result in a increase in false-positive rates. [25] The whitening transformation is applied to the data such that the data has zero mean and unit variance. The whitening method normalizes the fMRI voxel time series $V_i(t)$ by the following equation:

$$\hat{V}_i(t) = \frac{V_i(t) - \mu}{\sqrt{\sigma^2 + \epsilon}}, \tag{3.1}$$

where the normalized voxel intensity times series is $\hat{V}_i(t)$, $\mu = \frac{1}{T}\sum_{t=1}^{T} V_i(t)$ and $\sigma^2 = \sum_{t=1}^{T}(V_i(t) - \mu)^2$ are mean and variance of values of that voxel's intensity time series. T is number of time instances and $\epsilon > 0$ is a small number to prevent numerical instability.

3.1.3 Interpolation of fMRI Data For Increasing the Time Resolution

Voxel selection and whitening transformation (normalization) enable us to design algorithms, conduct experiments and analyses in more feasible time and complexity. As mentioned in the earlier chapters, TOL data has limited number of subjects and scans from short time periods. The lack of enough samples brings the problem of not being able to train the machine learning models to decode human brain. The decoding performance is intended to be increased by injecting generated informative data between the original data at original time instances.

In order to assess how the amount of information, which is introduced after generating samples with interpolation, entropy and frequency spectrum of the data sets are analyzed. Entropy is used to measure information gain as entropy is the average information production rate by a stochastic source of data. Therefore, entropy comparison between the real and generated data sets can be done to assess which data set carries more information.

Following entropy analysis, frequency spectrum is plotted to examine if the frequency spectrum of the interpolated data resembles the original one and the original nature of the fMRI data is preserved. Frequency spectrum of a signal is the range of frequencies contained by a signal. An intuitive understanding of the qualitative behaviour of the system can be revealed looking at the frequency spectrum of the signal. In this study, Fourier Transform will be used to find the frequency domain representation of the data set.

The main motivation of this study is to increase the number of time samples so that we have a sufficient number of the brain volumes to decode the cognitive tasks of human brain. We need to interpolate intensities over time in an intelligent way. Therefore, a

relation between time and intensity values should be found. Time information should be a part of the feature vector to achieve this. Discrete time values will be used to train interpolation model. The intensities for the time points in between will be queried and used in classification.

In TOL data set, each subject performs a set of experiments, which are called sessions. Subjects are asked to solve different puzzles having resting times between them. The puzzles are labeled as resting, planning and execution according to what the subject does at time of measurement. To make the time values in the input vector sufficient for training of regression models, each session is divided into puzzles and they are interpolated separately. Each puzzle is assumed to start on time point 0 and treated as if one scan was retrieved in a second.

The sessions are divided into puzzles using the fact that there are time periods that the subject is resting between the puzzles and each puzzle is composed of a continuous period of planning phase followed by a continuous period of execution.

The samples, which are generated by interpolation, have to be labeled as planning or execution. To explain labeling procedure, samples measured at time t and (t+1) are the observed time instances and generated samples are assumed to be in two groups divided by the mid sample. The samples generated in the [t,(2t+1)/2] are of the label of the sample measured at time t and the rest is labeled as the label of the sample measured at (t+1).

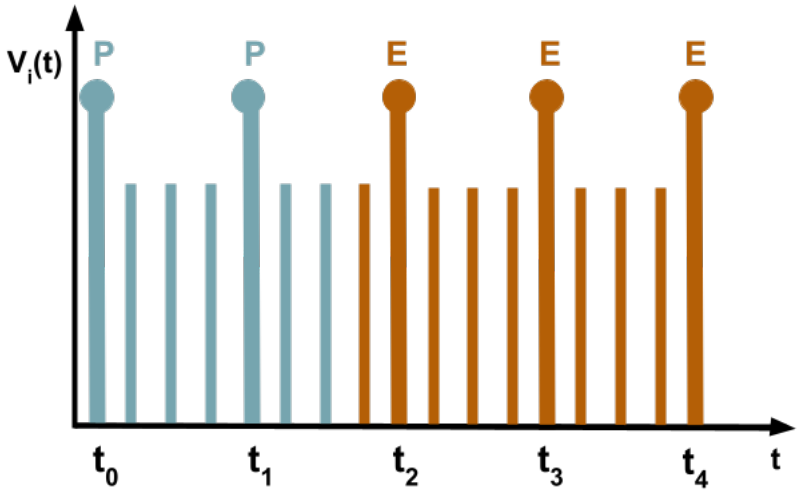


Figure 3.2: Voxel intensity vs. Time plot illustration to explain the labeling of the generated samples.

Figure 3.2 illustrates the labeling logic that is explained earlier in this Section. Samples at t_0, t_1, t_2, t_3 and t_4 represent the actual voxel intensity where as the lines in between are the interpolated intensities. P represents the label of the planning phase while E is for the label of the execution phase.

In this study, two methods to increase temporal resolution of the TOL data set are introduced.

3.1.3.1 Interpolation By Polynomial Regression

As we mention before, fMRI recordings resembles a nonlinear discrete function and cannot be modeled using linear regression. The nature of the data requires a nonlinear curve fitting method.

Figure 3.3 illustrates three puzzles from a voxel intensity time series. The figure shows that this time series can be fit to a polynomial function of degree 6 by examining the number of turning points in the plots for each puzzle.

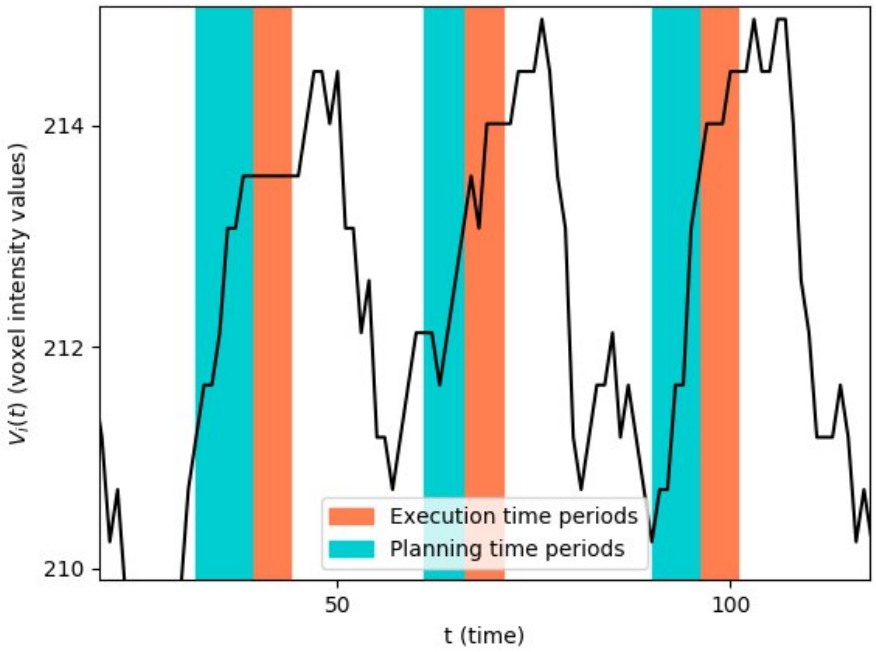


Figure 3.3: Voxel intensity vs. Time plot (Voxel 770, first 3 puzzles from session 3, subject 146).

Equation 3.2 formulates $V_i(t)$ as a k^{th} degree polynomial in t. $V_i(t)$ represents the voxel intensity value of i^{th} voxel at time t.

$$V_i(t) = a_0 + a_1 t + a_2 t^2 + \ldots + a_k t^k \tag{3.2}$$

Assuming that each voxel can be modelled independently from each other, the time series of a given voxel for a given puzzle is fit to a polynomial curve by minimizing the least squares error between the original samples and the results from polynomial function. The voxel intensity values at missing time instances are estimated for all puzzles separately and the interpolated data for each puzzle is concatenated to build the interpolated voxel session time series. For a session with 18 puzzles and 25000 voxels, $18 \times 25000 = 450000$ polynomial functions are estimated.

Observed time instance and voxel intensity value pairs are used for estimating the polynomial function. Predictions are done using the time values between the real

observation times as the polynomial curve provides a continuous representation for the voxel intensity time series. Generated samples are placed between the measured intensity values.

3.1.3.2 Interpolation By Neural Networks

In the previous section, an interpolation method using by minimizing the least squares error between the actual samples and a polynomial is proposed. Even though previously described method is promising, designing a more complex method have a potential to increase the performance even more.

In the previous method, it is assumed that the voxel intensity values over time can be modeled independently from each other. However, the spatial correlations also exist among the voxels. The fMRI data analysis cover the spatio-temporal relationship between a stimulus and the cerebral activation in fMRI. Even though the data has an apparent spatio-temporal nature, there are few proposed models based on this fact. [26, 12, 36] In this method, a spatio-temporal modelling method is proposed. Instead of having a model for each voxel-puzzle pair, a model per puzzle is trained. The estimation of voxel intensities is done by taking how voxels are located relatively to each other into account as well.

The coordinates of voxels provide spatial information about the proximity of voxel groups. In the suggested method, the feature vector is extended by adding voxel coordinates. The coordinates is normalization before being used.

A novel neural network model is proposed for building a nonlinear model to recover missing scans between the known brain volumes. The architecture has two network components as illustrated in Figure 3.4:

- **Neural Network 1:** A neural network layer that learns the spatial relations among the voxels using the voxel coordinates and then returns a new representation for the coordinates. The encoding step provides disentanglement of spatial and temporal weights. Neural Network 1 consists of a single fully connected

layer with 50 neurons. The new representation of the coordinates (x_i, y_i, z_i) is shown as $f(x_i, y_i, z_i)$ in Figure 3.4, where $f : \mathbb{R}^3 \rightarrow \mathbb{R}^{50}$. ReLu is selected as the activation function.

- **Neural Network 2:** A fully connected neural network that takes the measurement time t along with the encoded coordinates $f(x_i, y_i, z_i)$ as input, and then estimates a voxel intensity value $V_i(t)$ for the i^{th} voxel at the coordinate (x_i, y_i, z_i) and time t. This component has three fully connected layers with 100, 50 and 25 neurons. ReLu is used as the activation function.

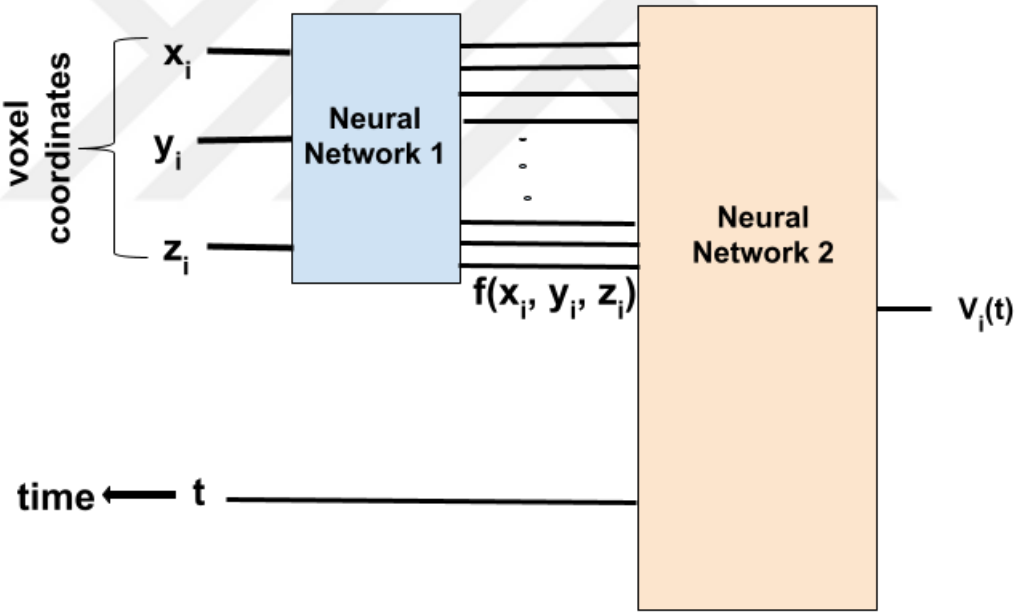


Figure 3.4: Neural network model for interpolation.

Each puzzle is modelled by training the neural network with the described structure. Interpolated puzzles are concatenated to create the interpolated session data.

3.1.4 Decoding the Planning and Execution Phases of TOL Game

Brain decoding in this study refers to predicting whether an fMRI sample was taken during planning or execution phases. After the voxel selection, whitening transformation on the original data, and data augmentation by temporal interpolation are performed, decoding the phases of complex problem solving is done. General idea in this step is to measure the effect of temporal interpolation on brain decoding performance.

In order to test the validity of the suggested interpolation methods, we train an SVM classifier with the original and interpolated data separately and test the classifier with the original data set. The amount of increase in the performances of the classifier can be considered as a measure of validities of the suggested methods.

3.2 Chapter Summary

In this chapter, we first give the motivation behind the proposed method. Then, We introduce the suggested method to increase the temporal resolution step by step. Voxel selection, temporal interpolation, normalization and brain decoding steps are explained in detail.

CHAPTER 4

EXPERIMENTS ON MEASURING THE EFFECT OF INTERPOLATION OF FMRI DATA ON BRAIN DECODING

In this chapter, the brain decoding performances for the original and interpolated data sets are measured and compared. Fourier and Shannon Entropy analysis is performed to analyze the decoding performances achieved.

4.1 Software and Hardware Configuration for Brain Decoding Experiments

The computer configuration is crucial to conduct experiments on this study because of the high dimensionality. It requires feasible RAM, CPU and GPU configurations. For polynomial model, utilizing CPU is generally sufficient while training a neural network with several layers requires GPU support to estimate that amount of parameters.

The server used for training processes has 32 GB of memory. Utilized graphics card is NVDIA GeForce GTX 1080 which has a 8 GB memory and memory speed of 10 Gbps. CPU is Intel Core i7-4930K CPU with processing speed of 3.40GHz.

The main programming language used in the study was Python to implement and prepare experiments fast. numpy, pandas, tensorflow-gpu, scikit-learn and scipy packages are used in the development of the experiment scripts. Neural networks are built utilizing tensorflow and other functionalities used such as polynomial regression and SVM is selected from scikit-learn. numpy and pandas are used to read data and do mathematical operations easily.

4.2 Experiments On TOL Data Set For Testing And Analyzing the Suggested Data Augmentation Model

In this set of experiments, SVM classifier is utilized for examining the effect of interpolation by the proposed methods. fMRI samples are classified into two cognitive states, namely planning and execution.

Voxel selection is applied to the data set as a first step. 25000 voxels are selected as in [2] for comparable results and in addition to that, 6000 voxels are selected to get faster results while determining the parameters for the interpolation. Figure 4.1 presents a histogram for the average selected voxel count per anatomic regions of the brain.

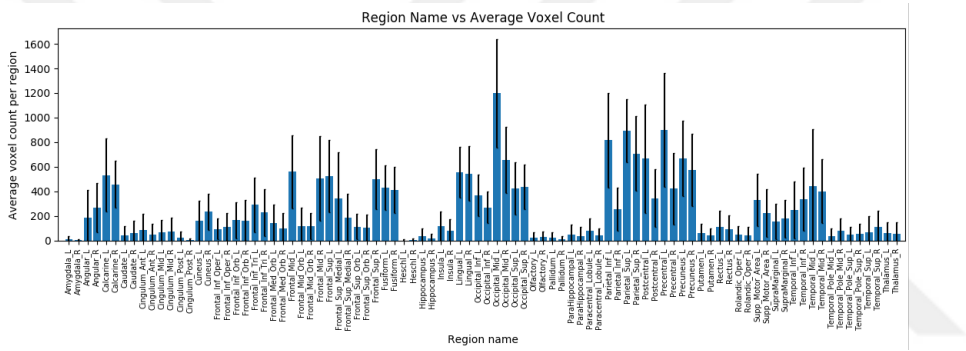


Figure 4.1: Average number of voxels selected from each anatomical region across all subjects.

Each fMRI data acquisition session consists of solving a puzzle. First, the sessions are divided for each puzzle to be used in k-fold cross validation. 8-fold cross validation is used to compute model accuracy. In each run of train and test, seven of the puzzles are selected to fit the model and the remaining one is used to test the model. The mean of the accuracies retrieved from each run is written down as the performance of the data set used for training.

In order to compare the brain decoding performances, a baseline classification is done by training an SVM using the original fMRI data without any interpolation. The prediction accuracies of this baseline experiment are listed in Table 4.1,

Table 4.1: Brain decoding accuracy results for the original fMRI data.

#voxels	normalized	not normalized
6000	**0.8489**	0.7217
25000	0.8483	0.7506

The first interpolation method introduced in Chapter 3 is the polynomial regression. A polynomial function or order 6 and 8 is estimated for the both fMRI data sets with reduced voxel numbers, 6000 and 25000.

The second proposed method is a novel neural network architecture to interpolate the fMRI data by regression. The same reduced data sets with 6000 and 25000 voxels are experimented for their impact in the brain decoding accuracy. The result with the best classification accuracy is achieved by the suggested model as shown in Table 4.4. The model receives normalized coordinate and time information at the input. The model has a hidden layer with 50 neurons to learn the spatial relations among the voxels, and three fully connected hidden layers with 100, 50 and 25 nodes for the voxel intensity value prediction that expects the encoded coordinates and time at the input.

Number of epochs is 500, which is selected according to the sum of absolute errors in each epoch. Figure 4.2 shows the sum of absolute errors and it can be seen that the error stops decreasing around 500^{th} epoch.

Learning rate is selected as 0.01 as the start value. Looking at the errors for each epoch shown in Figure 4.2, the learning rate has been decreased gradually during the training. ReLu is the selected as activation function.

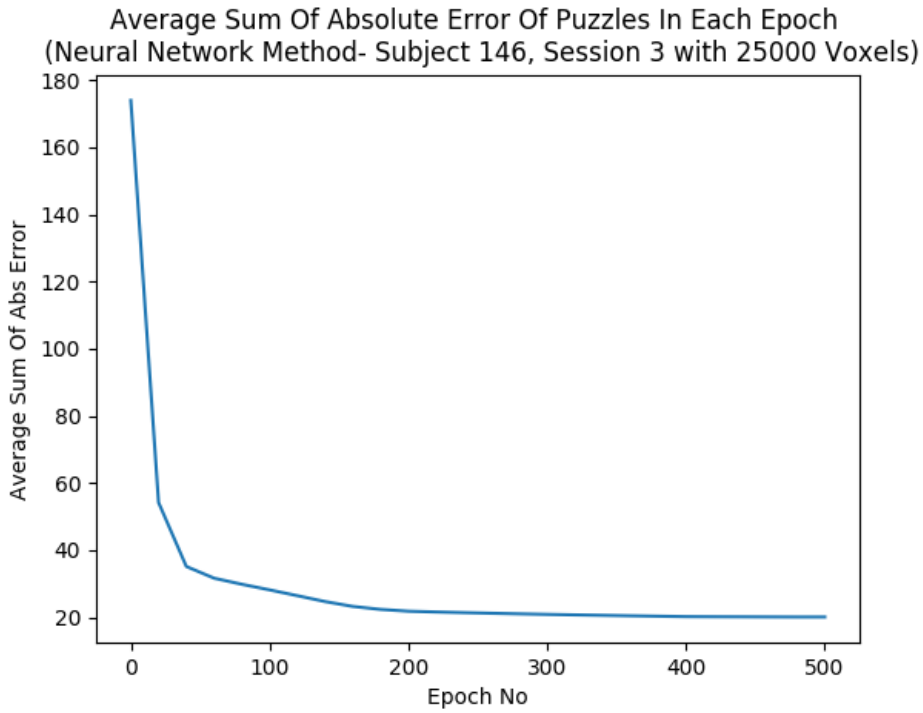


Figure 4.2: Average Sum of Abs Error of Puzzles In Each Epoch (NN Method - Subject 146, Session 3 with 25k Voxels).

After data generation, the puzzle indices for train and test is determined for each run of 8-fold cross validation. The train puzzles are taken from generated data and test puzzle are from original data. The mean of the decoding performances can be found in the Table 4.2 and 4.4,

Table 4.2: Brain decoding accuracy results for the fMRI data interpolated by the polynomial regression.

polynomial degree	#voxels	normalized	not normalized
6	6000	0.8684	0.8075
6	25000	**0.8715**	0.8075
8	6000	0.8666	0.8066
8	25000	0.8680	0.8246

Table 4.3: Brain decoding accuracy results for the fMRI data interpolated by the proposed neural network method.

#voxels	normalized	not normalized
6000	0.8663	0.8304
25000	**0.8806**	0.8515

Table 4.1, 4.2 and 4.4 report the brain decoding performances for the original and interpolated fMRI data sets. Table 4.1 shows that the baseline performance for the brain decoding is 85%. We achieve 87% when the temporal resolution is increased using the polynomial interpolator of degree 6 on 25000 voxels as listed in Table 4.2. The feature vector with 25000 voxels gives a sligtly better performance than using 6000 voxels. In addition, Table 4.2 shows polynomial of degree 6 reaches a better performance than degree 8. It means that degree 6 provides a better modelling of the signal than degree 8. The highest performance, which is 88%, is achieved using the neural network interpolator as reported in Table 4.4. This shows that representing the voxel signal as a higher-order non linear function improves the performance.

Table 4.4: Brain decoding accuracy results for the fMRI data interpolated by the proposed neural network method.

#voxels	normalized	not normalized
6000	0.8663	0.8304
25000	**0.8806**	0.8515

Before conducting experiments on the suggested neural network interpolator, a simpler neural network architecture is used to perform temporal interpolation of the original fMRI data. This neural network has 3 fully connected layers with 60, 40, 20 neurons. ReLu is used as the activation function and the number of epochs is selected as 400 according to the sum of absolute errors in each epoch. The main difference

from the suggested method here is that this architecture does not encode the voxel coordinates. Here input layer expects an input vector $[x_i, y_i, z_i, t]$, which consists of coordinates of the i^{th} voxel and the time t as illustrated in Figure 4.3.

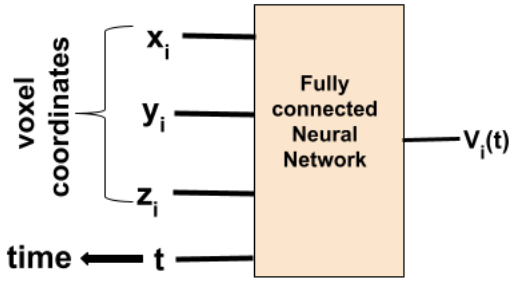


Figure 4.3: The simple neural network that is experimented before experimenting our suggested method which is described in Section 3.1.3.2.

The fMRI data interpolated using the simple neural network results in the lowest brain decoding performance among all the methods we experiment. The performance is reported as 84% in Table 4.5 while the proposed neural network architecture achieves 88%. This proves that the disentanglement of space and temporal weights is necessary to improve the performance. The first component of the proposed neural network shown in Figure 3.4, which encodes the voxel coordinates and learns the spatial relations among the voxels, plays a key role in modelling the TOL data.

Table 4.5: Brain decoding accuracy results for the fMRI data interpolated by the simple neural network method illustrated in Figure 4.3.

#voxels	normalized	not normalized
25000	**0.8420**	0.7298

4.2.1 Analysis of the Interpolated fMRI Data

In this section, we analyze and compare the original and interpolated fMRI data in terms of their information content and frequency domain spectrum.

Figure 4.4, 4.5, 4.6, 4.7 and 4.8 show Voxel intensity vs. Time plot of a randomly selected voxel. The parts with white background correspond to the resting state, the orange parts show the planning state and blue back-grounded parts mean that subject is in planning state. The plots are from data sets with 25000 voxels.

The voxel intensity values generated for an individual voxel do not depend on the selected voxel number for polynomial regression, because each voxel has its own regression model for generation. Polynomial regression with degree 6 for 25000 selected voxels provides an increase in classification performance around 2% which was reported in Tables 4.1 and 4.2.

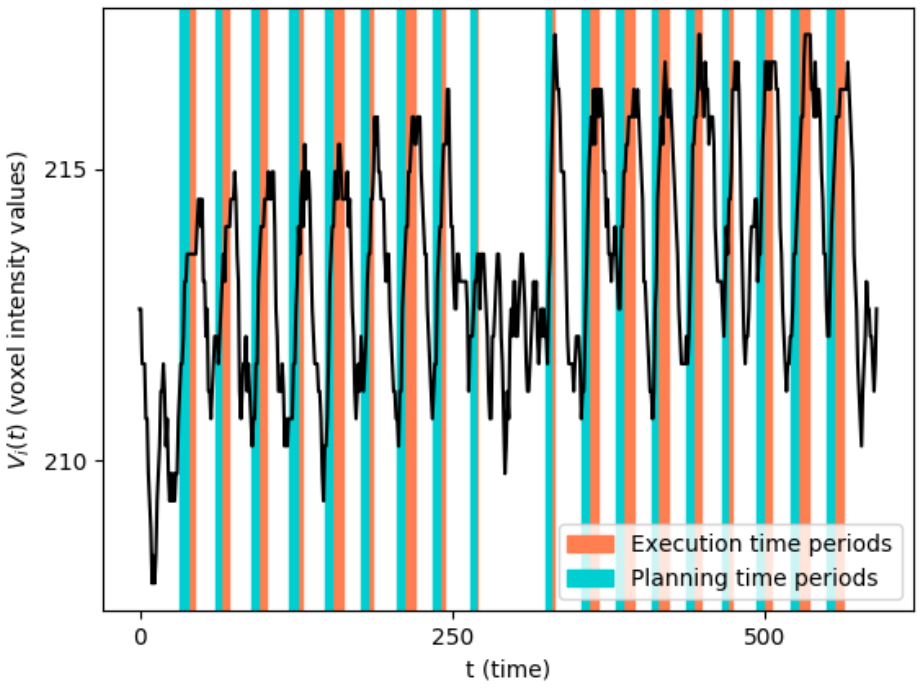


Figure 4.4: The original voxel intensity values vs. Time plot of voxel with id 770.

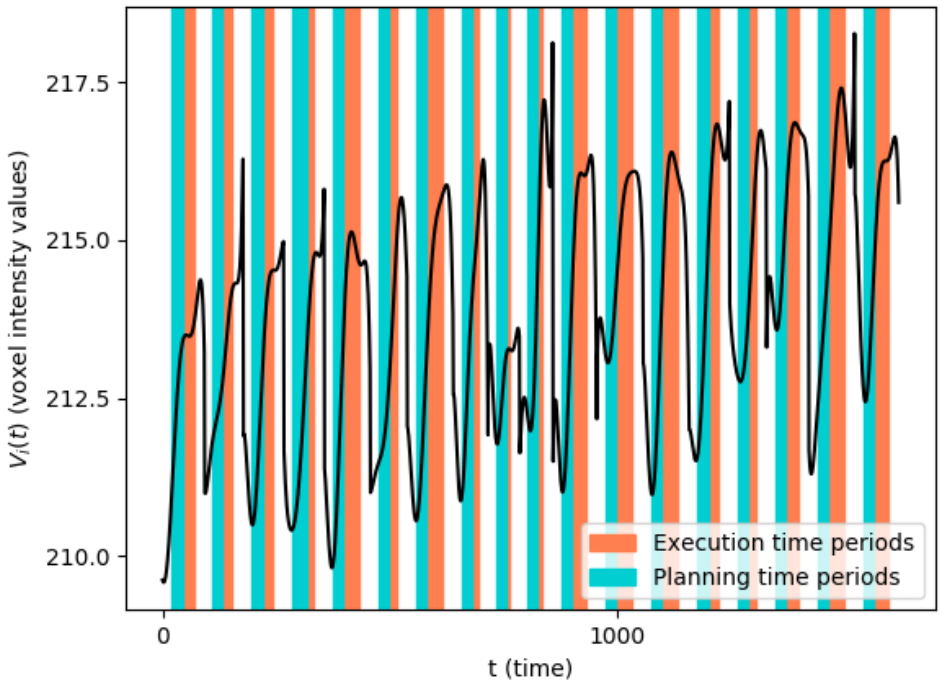


Figure 4.5: The voxel intensity values vs. Time plot of voxel with id 770 after improving temporal resolution by polynomial regression of degree 6.

As seen in the Figure 4.4 and 4.5, the polynomial interpolation performs smoothing on the original signal. Representing the signal as a polynomial curve of degree 6 has a higher generalization performance compared to the original signal and it avoids overfitting.

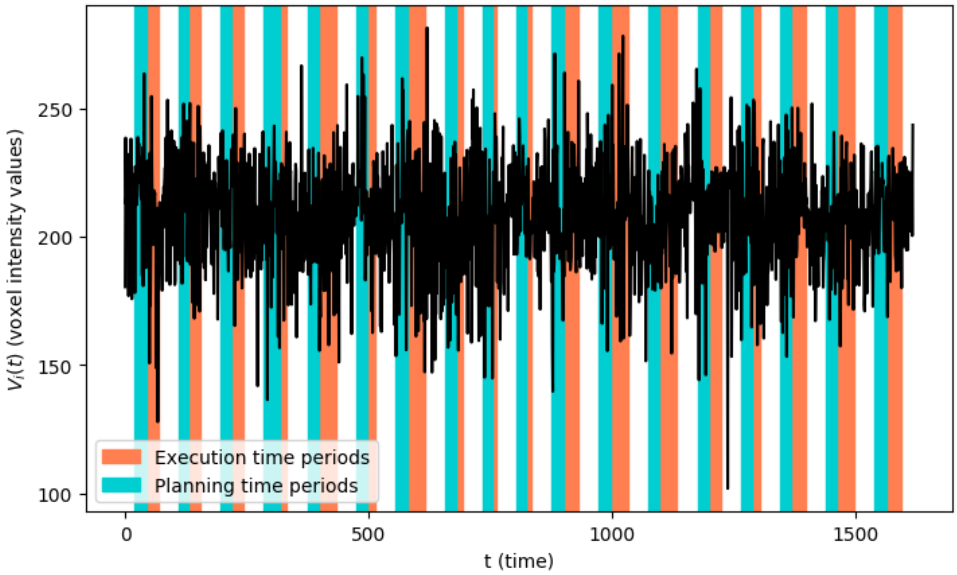


Figure 4.6: The voxel intensity values vs. Time plot of voxel with id 770 after improving temporal resolution by the method using neural networks.

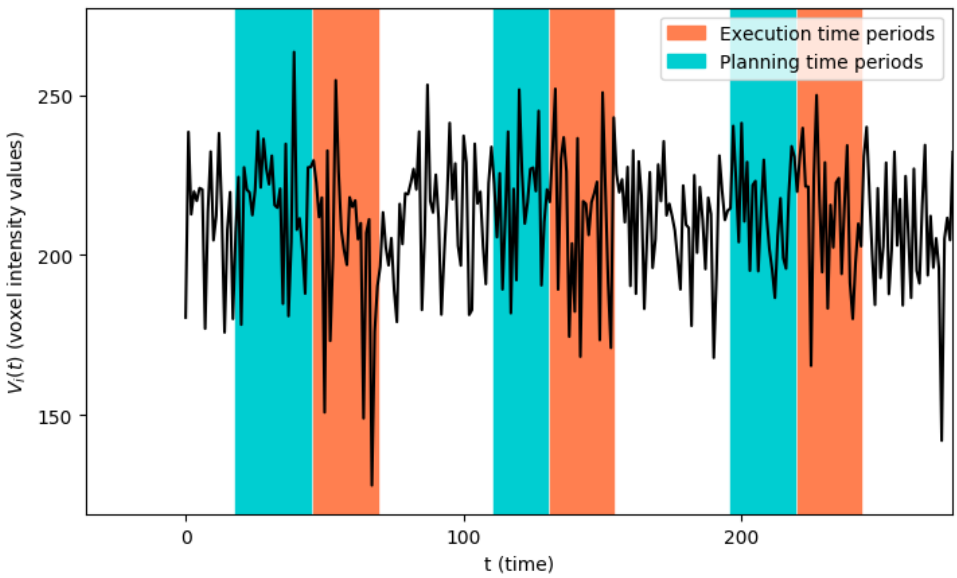


Figure 4.7: The voxel intensity values vs. Time plot of voxel with id 770 after improving temporal resolution by the method using neural networks for the first 3 puzzles only.

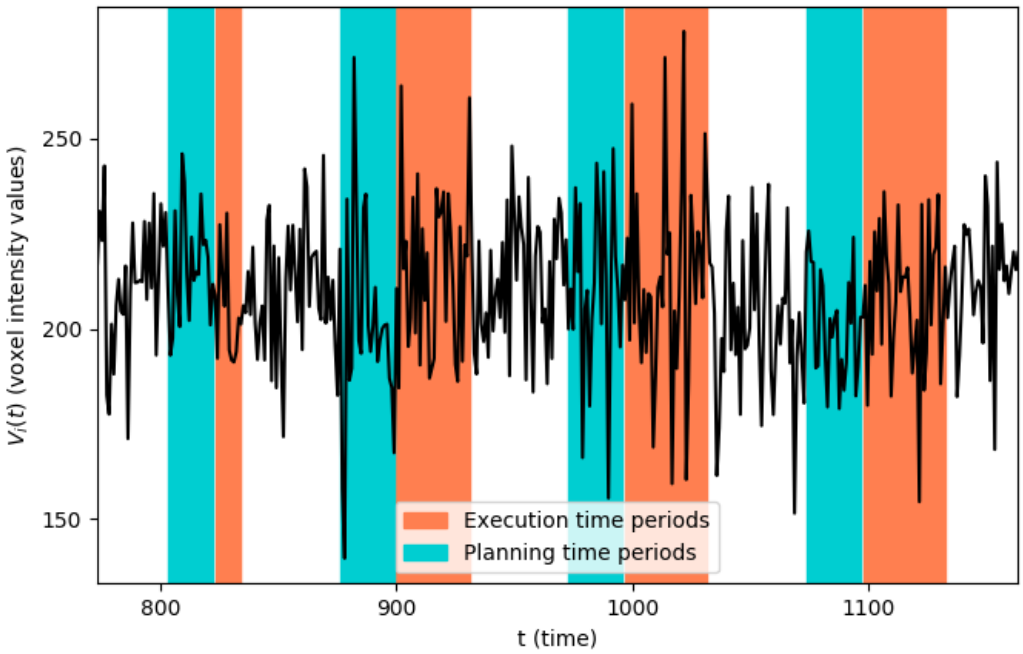


Figure 4.8: The voxel intensity values vs. Time plot of voxel with id 770 after improving temporal resolution by the method using neural networks for the puzzles with id 10-11-12-13 only.

As reported in Table 4.4, the proposed interpolation by neural network with a novel architecture gives the highest brain decoding performance among all of the performances noted. The voxel intensity vs. Time plot, $V_i(t)$ vs. t, of voxel 770 after neural network interpolation is shown in Figure 4.6, 4.7 and 4.8. As seen, it has a nonlinear nature.

After examining these plots, simpler architectures with smaller depth and number of neurons may be considered to check if there is an overfitting problem. However, the most notable performances are achieved by this setting in terms of brain decoding experiments. Analyzing the interpolated voxel time series shows that this architecture adds a high degree of nonlinearity to the fMRI measurements. Therefore, a better performance has been achieved. This observation can be examined in depth by looking at the Fourier Transform plots and entropy comparisons of the original and interpolated

brain volumes.

In order to compare the nature of the original and interpolated fMRI data, plots for shorter time periods are provided for visual inspection in Figure 4.7 and 4.8. This enables us to analyze the puzzles in detail.

All of the reported decoding performances show that the normalization of the fMRI time series increases classification performance notably. Noise coloration in fMRI data caused by physiological and physical effects outside of the experiment may cause false-positives. The whitening transformation gets rid of those effects.

4.2.1.1 Entropy Analysis

Entropy is used to measure the number of possible states to a system. In intelligent systems, the information is modelled into states according to reconfigurations of its components. This study focuses on the information retrieved from the brain in the form of fMRI data. Brain as an intelligent system utilizes the information by creating models of sensory input through readjustments of neural connections [30].

Brain entropy gives us the predictability of voxel signals over time as it does not measure the number of states directly. It provides us an estimation which has a very close relation to the number of possible states in the brain namely predictability of the behaviour of the voxel signals. In this study, information density introduced by Shannon is used to estimate predictability since they are closely related [32]. Less predictable voxel time series has higher entropy since each data point introduces new information while low entropy time series has a repeating pattern over time making it predictable.

Neuroscience studies discovered that a collection of anatomic regions coordinate to form a cognitive task, for instance the complex problem solving. Hence, in this study, we stimate the anatomic region level entropy to analyse the classification results. For a region participating the complex problem solving task more, voxel BOLD signal intensities are expected to have a pattern over time. Therefore, they produce lower

entropy compared to less active anatomical regions as their voxel time series have a random nature. [10].

As described above, we expect to see lower entropy for the data sets generated by the proposed methods since higher decoding performance is achieved using the classifiers trained with them.

Before moving onto entropy results and comparison, let us formulate the static entropy estimation for each anatomic region.

fMRI BOLD signals for a Complex Problem Solving session is a set of voxel time series of length n representing the neural activity. BOLD values measured for a voxel V_i are represented as time series $V_i(t)$. Averaging the time series of the voxels located in a region gives the representative time series for the region which we will refer as $V_r(t)$. n_r represents the number of voxels in a region r [10].

$$V_r(t) = \frac{1}{n_r} \sum_{\forall V_i \in r} V_i(t) \tag{4.1}$$

Kernel probability density estimation method is used to estimate the probability density function, $P(V_r)$ for a given region [10].

$$P(V_r/r) = \frac{1}{nh} \sum_{t=1}^{n} K(\frac{V_r - V_r(t)}{h}) \tag{4.2}$$

where n is the number of time samples for a session, V_r is the representative time series for a region r, K is the kernel smoothing function, and h is the bandwidth size.

Finally, the estimated probability density function is used to calculate the region entropy for a given region r:

$$H(X_r) = - \sum_{\forall t \in V_r(t)} P(V_r) log_2 P(V_r) \tag{4.3}$$

In the study [7], the regions with the lowest static entropy are reported. We select a subset of 10 anatomic regions from the listed regions, which are right superior parietal gyrus, left superior parietal gyrus, left medial orbitofrontal gyrus, right Precuneus, left calcarine, right calcarine, left angular gyrus, right lingual gyrus, right cuneus,

and left cuneus to estimate the entropy values for our data sets. These regions are also mentioned to be the most active regions in the previous neuroscience studies [16, 3].

The region entropies are estimated for each session for a given subject. Figure 4.9, 4.10, 4.11, 4.12 and 4.13 show the region entropy estimations for different data sets for TOL experiment.

First, we select the samples labeled as planning phase and estimate the regional static entropy as formulated before in Equation 4.1, 4.2 and 4.3. Following that, execution time instances are analyzed separately.

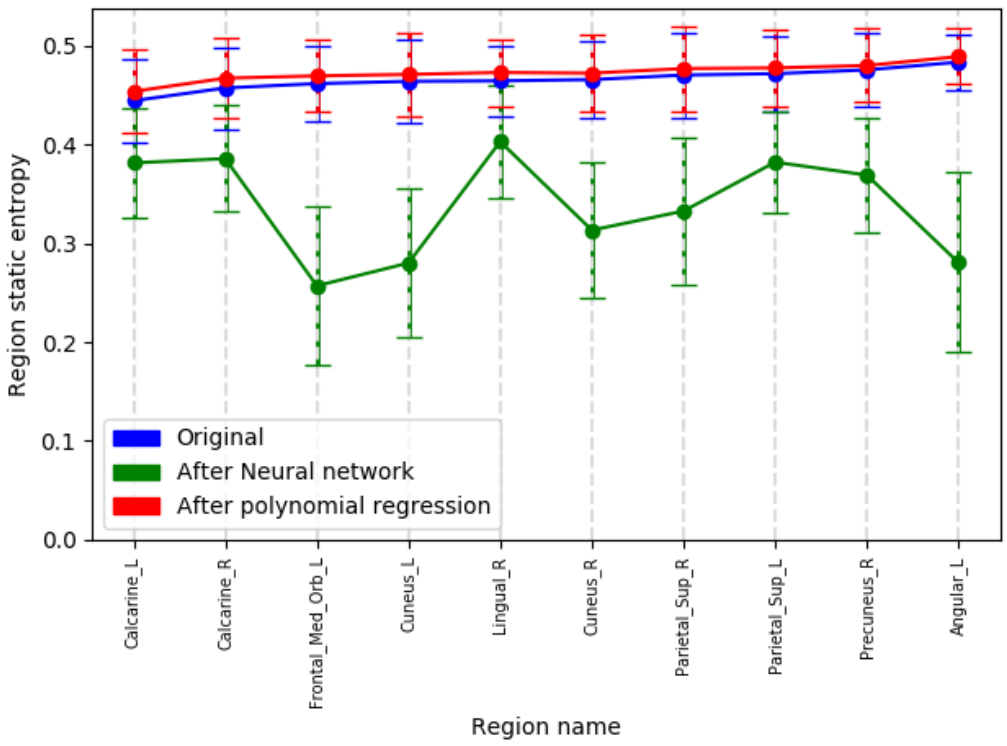


Figure 4.9: Region entropy estimations for samples labeled as planning phase. Averaged for all sessions and subjects, calculated using all data sets: the original fMRI data, the interpolated fMRI data by the polynomial interpolation of degree 6 and the interpolated fMRI data by the proposed neural network method.

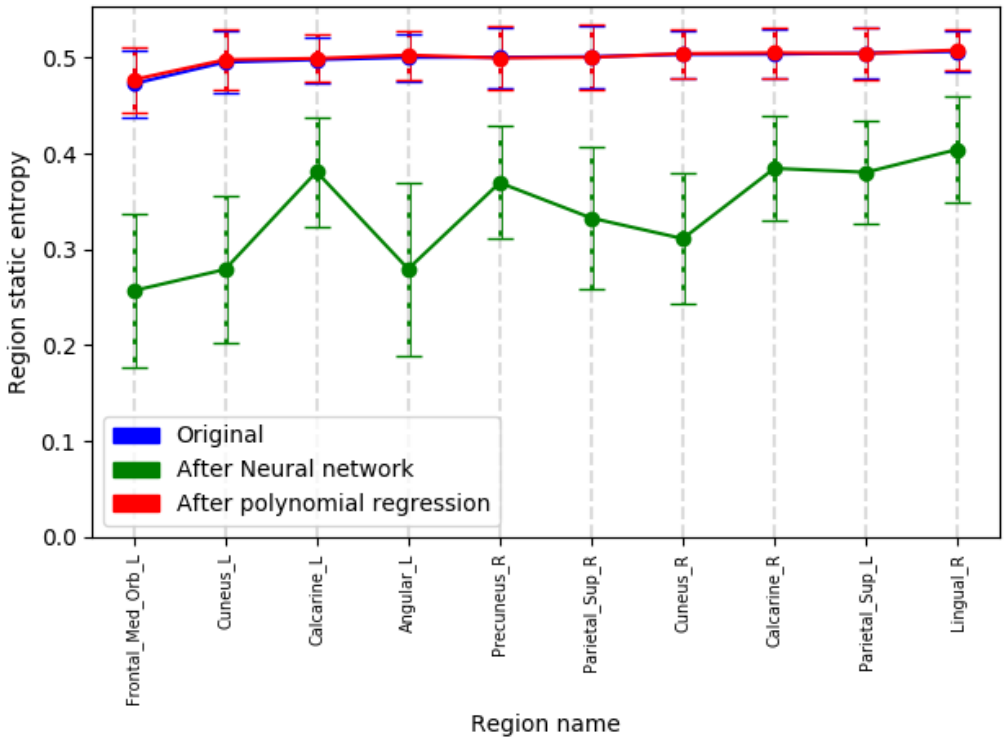


Figure 4.10: Region entropy estimations for samples labeled as execution phase. Averaged for all sessions and subjects, calculated using all data sets: the original fMRI data, the interpolated fMRI data by the polynomial interpolation of degree 6 and the interpolated fMRI data by the proposed neural network method.

Secondly, an entropy estimation is performed on the full time series, without selecting the planning or execution phases. Following figures illustrate the results obtained from these experiments.

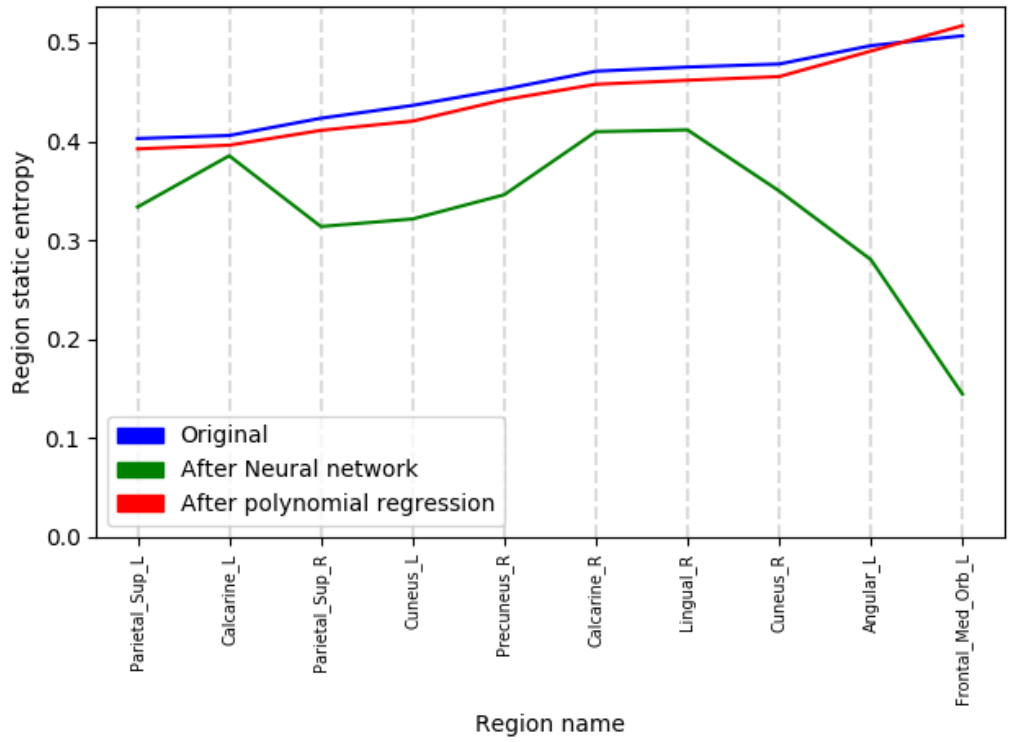


Figure 4.11: Region entropy estimations for the session 5 of subject 175, calculated using all data sets: the original fMRI data, the interpolated fMRI data by the polynomial interpolation of degree 6 and the interpolated fMRI data by the proposed neural network method.

Figure 4.11 exhibits the entropy estimation for subject 175 who is an expert participant. It shows a similar range for the entropy estimations reported in Figure 4.9 and 4.10. We see that neural network and polynomial interpolation increase the information content of the fMRI data.

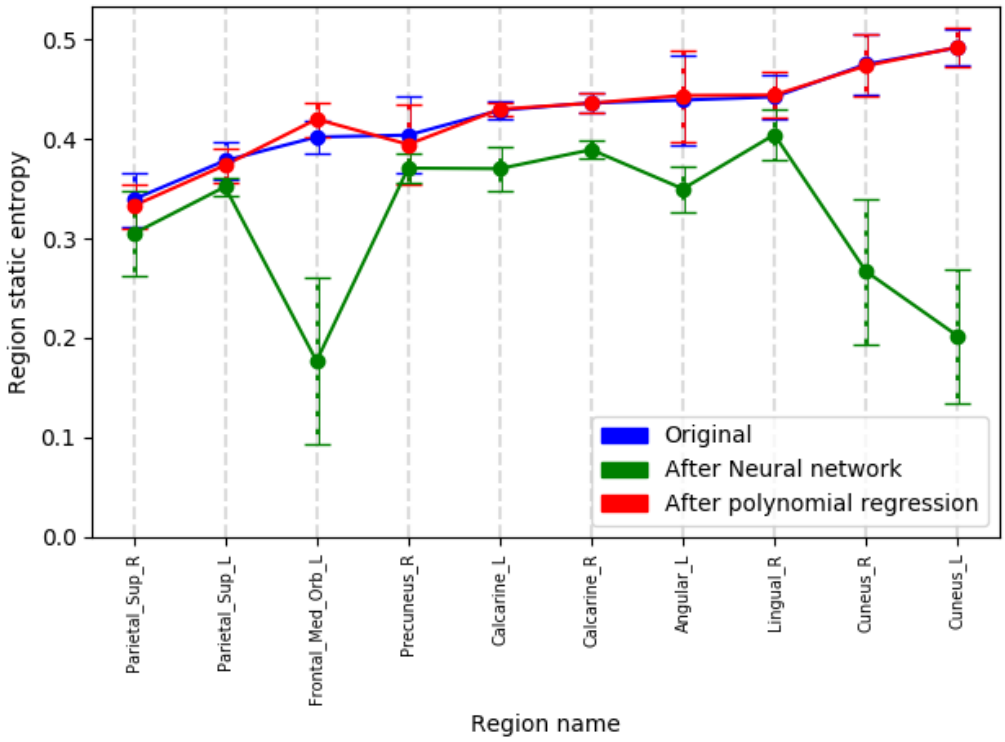


Figure 4.12: Region entropy estimations averaged for all sessions of subject 146, calculated using all data sets: the original fMRI data, the interpolated fMRI data by the polynomial interpolation of degree 6 and the interpolated fMRI data by the proposed neural network method.

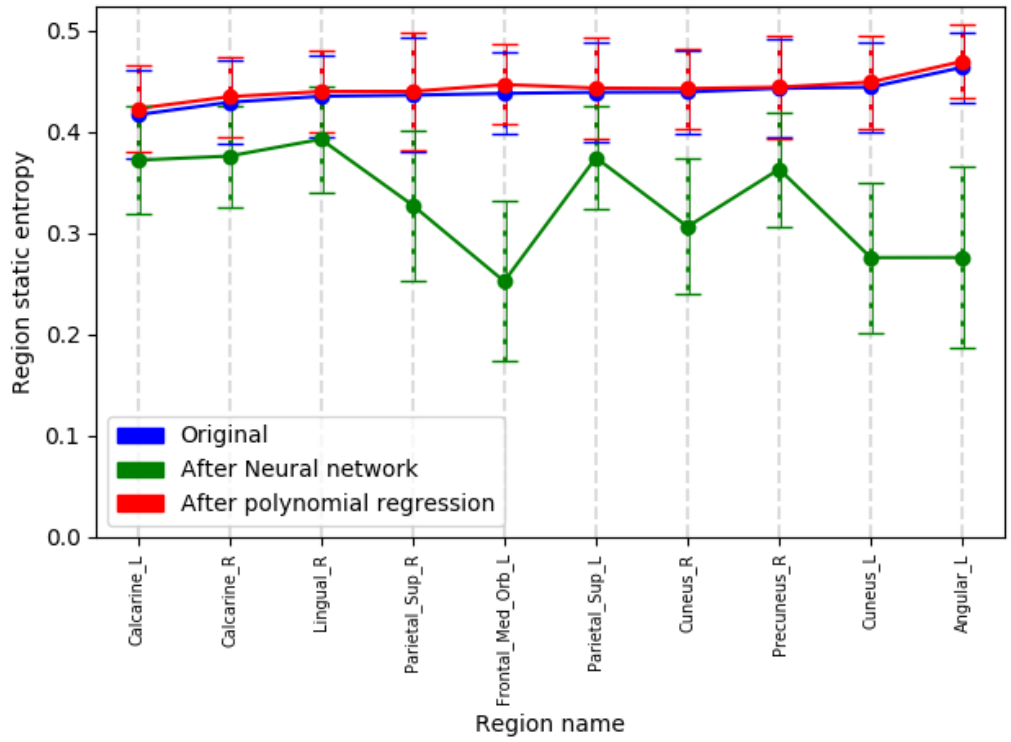


Figure 4.13: Region entropy estimations averaged for all sessions and subjects, calculated using all data sets: before interpolation, after polynomial interpolation (degree=6) and after neural network interpolation.

As seen in the Table 4.1, Table 4.2 and Table 4.4, there is an increase in the classification performance after interpolating the data. Figure 4.9 and 4.10 show very close entropy values for the original fMRI data and the fMRI data interpolated by the polynomial model. The plots also show that interpolation performed using neural network method resulted in a dramatic decrease in region level entropy. Figure 4.11, Figure 4.12 and Figure 4.13 illustrate a similar result for the analysis from the data with all phases.

Table 4.6, Table 4.7 and Table 4.8 can be seen for a detailed analysis as they clearly list the estimated values. It proves the entropy values are consistent with the classification results. Neural network interpolation increases classification results noticeably and it is seen that it has lower entropy values compared to the other data sets. Polynomial

regression achieves a negligible increase in classification performance so it is pretty close to original data set in terms of entropy.

Table 4.6: Region Entropy Estimation (Averaged for all sessions and subjects) (bits/sample).

	Original	Polynomial Int.	NN Int.
Calcarine_L	0.4167	0.4228	0.3719
Calcarine_R	0.4290	0.4345	0.3759
Lingual_R	0.4350	0.4397	0.3925
Parietal_Sup_R	0.4361	0.4398	0.3275
Frontal_Med_Orb_L	0.4378	0.4466	0.2522
Parietal_Sup_L	0.4389	0.4431	0.3743
Cuneus_R	0.4392	0.4426	0.3062
Precuneus_R	0.4428	0.4440	0.3630
Cuneus_L	0.4440	0.4490	0.2757
Angular_L	0.4636	0.4695	0.2758

Table 4.7: Region Entropy Estimation for Planning Phase (Averaged for all sessions and subjects) (bits/sample).

	Original	Polynomial Int.	NN Int.
Calcarine_L	0.4445	0.4540	0.3816
Calcarine_R	0.4575	0.4674	0.3859
Frontal_Med_Orb_L	0.4619	0.4697	0.2570
Cuneus_L	0.4642	0.4712	0.2801
Lingual_R	0.4647	0.4731	0.4031

Table 4.8: Region Entropy Estimation for Execution Phase (Averaged for all sessions and subjects) (bits/sample).

	Original	Polynomial Int.	NN Int.
Frontal_Med_Orb_L	0.4728	0.4771	0.2568
Cuneus_L	0.4954	0.4979	0.2790
Calcarine_L	0.4980	0.4993	0.3809
Angular_L	0.5004	0.5027	0.2796
Precuneus_R	0.5004	0.4998	0.3695

4.2.1.2 Fourier Transform Plots and Analysis

The Fourier Transform decomposes a function into a sum of sinusoidal basis functions. Fourier transform is one of the major methods to compute frequency domain representation of a signal. Fourier transform of a continuous voxel signal $v(t)$ is computed as follows where f is the sampling frequency:

$$\mathscr{F}\{v(t)\} = F_i(f) = \int_{-\infty}^{\infty} V_i(t) e^{2\pi i f t} dt \tag{4.4}$$

In our case, we have discrete intensity values representing voxel signals that's why discrete Fourier transform is utilised. It is computed as below where T is the number of time samples:

$$\mathscr{F}\{V_i(t)\} = F_i(f) = \sum_{i=1}^{T} V_i(t) e^{2\pi i f t} dt \tag{4.5}$$

In this section, frequency domain representation plots for the signals are analyzed to qualify the frequency content of the voxel time series. Figure 4.4, Figure 4.5 and Figure 4.6 compares the analyse the consistency of the brain decoding performances from the original and interpolated fMRI data. Fourier transform gives us important information about the signal's nature.

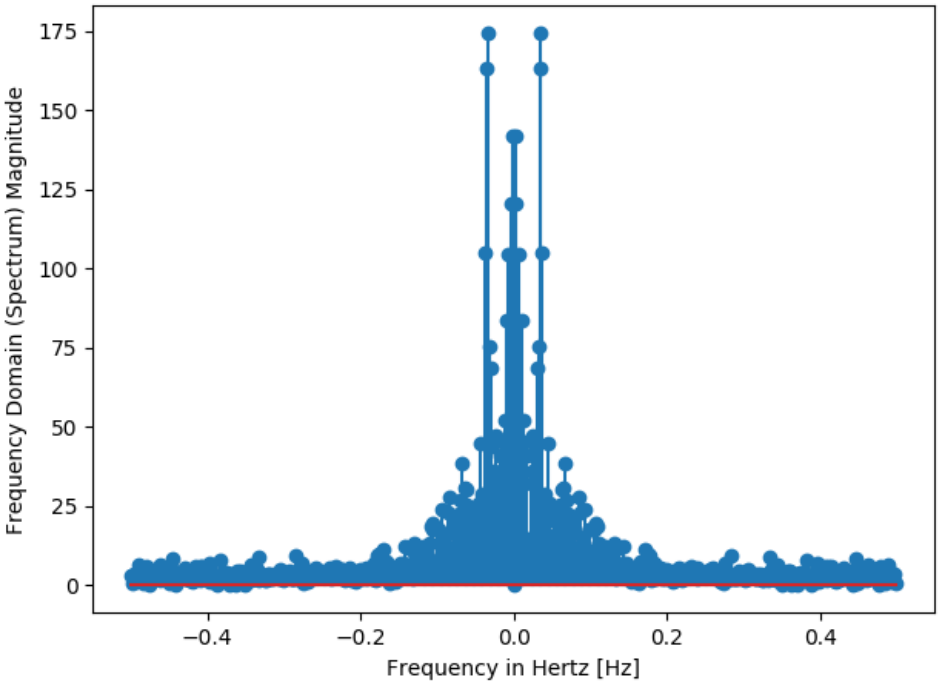


Figure 4.14: The Fourier Transform of the original voxel intensity vs. Frequency plot of voxel with id 770.

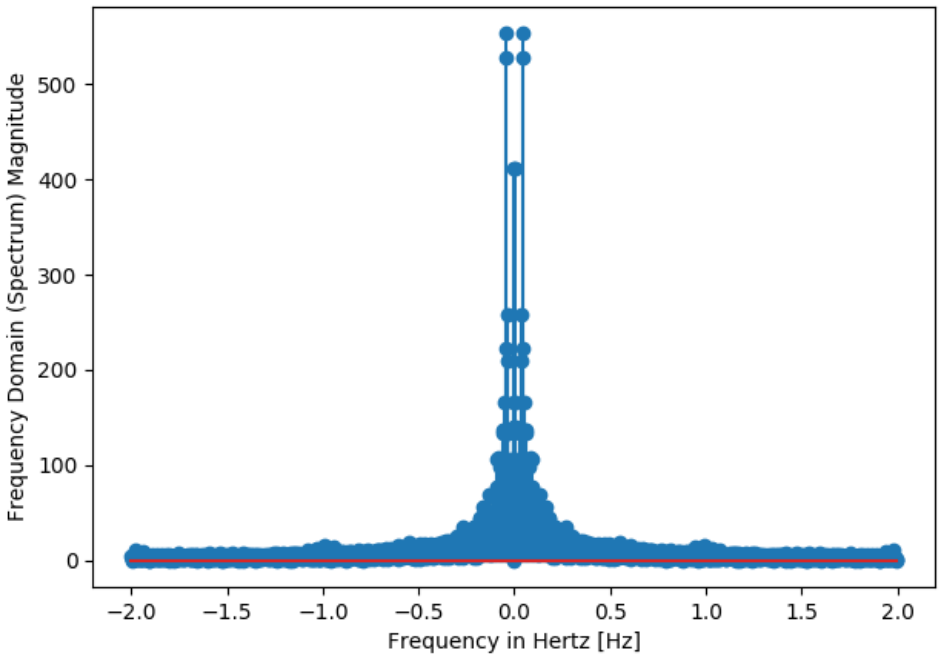


Figure 4.15: The Fourier Transform of voxel intensity vs. Frequency plot of voxel with id 770 after improving temporal resolution by the polynomial interpolation method.

Figure 4.14 and Figure 4.15 plots show the frequency spectrum of the original signal and the interpolated signal using polynomial regression with degree 6 for voxel 770 of subject 146 during session 3. Recalling the classification results presented, the classification performances are pretty close to each other for these data sets. The data set interpolated by polynomial regression with degree 6 adds a slight performance improvement. As seen in the plots provided for Fourier transforms, the frequency domain representation for the signals have a common shape. Only some frequency values are introduced in the interpolated one preserving the same shape while not introducing any non linearity.

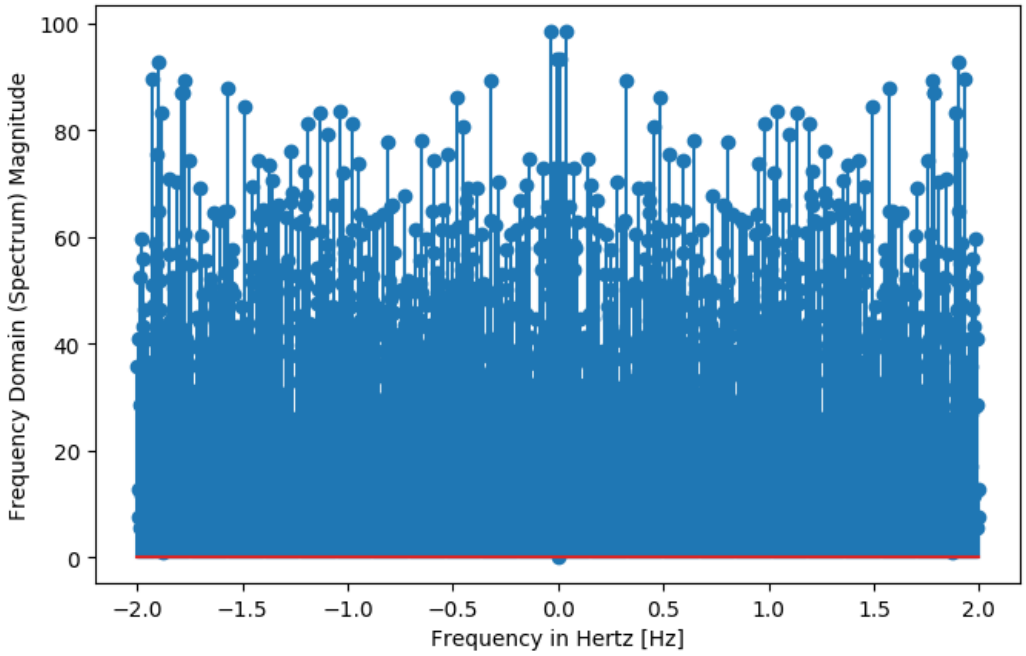


Figure 4.16: The Fourier Transform of voxel intensity vs. Frequency plot of voxel with id 770 after improving temporal resolution by the neural network method.

Figure 4.16 is created for the interpolated fMRI data by the suggested neural network method. As shown in the signal plot itself as Figure 4.6, the generated signal has a higher degree of nonlinearity compared to other data sets, which leads a better brain decoding performance. Since neural network introduced by this study has a great amount of parameters compared to polynomial regression method, it can fit a complex function to the data. As seen in the Figure 4.16, this method introduces a wide range of different frequencies resulting in a higher degree of nonlinearity for the data.

4.2.1.3 Complexity and Scalability

TOL data has a high spatial resolution. In the original fMRI recordings, each brain volume consists of 185405 voxels. Since the interpolation methods introduced in this

study have high computational complexity with many parameters to be estimated. It is not feasible to use a feature set with many features.

The time it takes to train the proposed models is pretty dependent on number of voxels. We can roughly calculate number of parameters to be estimated for each method. We recall that the neural network interpolator is represented with 2 components in Figure 3.4. The component that learns the spatial relations among the voxels takes an input with 3 features and trains 50 neurons. The second component, which expects the encoded representation of the voxel coordinates and time, has 3 fully connected hidden layers with 100, 50 and 25 neurons. It outputs the predicted voxel intensity value for the given voxel location and time. In each epoch, $3*50+51*100+100*50+50*25$ parameters for weights and $1*50\ +1*100\ +1*50\ +\ 1*25$ parameters for bias are to be estimated in the neural network model. Recalling that we use 500 epochs for training the neural networks, this amount of parameters are estimated 500 times.

The set of input vectors consist of the all combinations of the observation times and voxel coordinates. Therefore, the number of voxels affects the time we update the parameters during an epoch. Obviously, training takes more time as the voxel set gets bigger. Number of samples is also a multiplier for the duration of training.

For polynomial regression, the method fits a model for each voxel's signal. That makes $polynomial function degree\ +1$ parameters to estimate for each voxel. The total number of parameters to estimate in the polynomial interpolation method is $(polynomial\ function\ degree + 1) * (number\ of\ voxels)$. Therefore, the methods are not scalable in terms of feature set size. Table 4.9 exhibits the average time for generating samples for subject 146-session 3 data using different methods.

Table 4.9: Total time spent on data generation for subject 146 session 3 data.

Method	# of voxels	Data generation duration
Neural network interpolation	6000	314 seconds
Neural network interpolation	25000	1251 seconds
Neural network interpolation	185405	Hardware was not enough to compute
Polynomial interpolation	6000	86 seconds
Polynomial interpolation	25000	361 seconds
Polynomial interpolation	185405	2456 seconds

According to the results presented in Table 4.9, the number of voxels is almost in linear relationship with the run time which includes training the generator model and generating samples. It can be seen that sample generation for only one session of one subject took at least 86 seconds for the polynomial regression and at least 314 seconds for the neural network model. According to the classification results, 25000 voxels give the best result with neural network model and it is taking 1251 seconds. Recalling that we have 18 subjects with 4 sessions each, we multiply the reported run times with 72 to calculate the approximate time it takes to complete the data augmentation for the whole data. It is obvious that this algorithms take too long for the high dimensional feature spaces and it is not feasible to scale the feature set up. It is also reported that using all of the voxels in feature set is not possible for the neural network model.

Due to the reasons mentioned in above, the methods are not scalable in terms of the number of samples. We update parameters for each sample in an epoch. Therefore, as the number of brain volumes gets bigger, the training will be slower. Also, the methods do not necessarily need to be scalable with respect to number of samples, since we propose the data augmentation methods because there is not enough samples to train a classifier in the original fMRI data. If we had the sufficient number of samples in the data to prevent the Curse of Dimensionality problem, the brain activation could be decoded to complex problem solving phases without generating samples.

4.3 Chapter Summary

In this chapter, the effect of the temporal interpolation on brain decoding performance is presented. The reported results are discussed by using Fourier and Shannon Entropy analysis.

Table 4.10: Brain decoding performance summary of the proposed method.

Method	Brain decoding performance
Baseline	0.8489
Polynomial Interpolation	0.8715
Neural Network Interpolation	**0.8806**

Table 4.10 summarizes the highest performance from each experiment. Baseline performance corresponds to the decoding performance for the original fMRI data. Polynomial interpolation and neural network results correspond to the results of the suggested method.

CHAPTER 5

CONCLUSION

In this study, we focus on improving the brain decoding performance by enhancing temporal resolution of fMRI data set. We propose two novel methods for temporal interpolation to reduce the effects of the Curse of Dimensionality problem, and discuss the results observed through the experiments conducted. The suggested model is verified and validated in an fMRI data set, while the subject solve a complex problem, they played the Tower of London (TOL) game.

5.1 Summary

In this study two interpolation methods are introduced following the application of standard data pre-processing methods. These methods are discussed and justified with the experiments, results and analyses.

- Preprocessing Step:

  - Since the fMRI data, for the TOL game experiment, has a high spatial resolution, it is not feasible to keep all of the voxels in the feature set. Besides, irrelevant voxels in the feature set may lead to poor generalization performance causing the overfitting problem in both interpolation and classification steps. 25000 and 6000 voxels are selected to create two separate data sets with reduced voxel number utilising ANOVA voxel selection method.

  - The feature vectors are normalised such that the data set has a zero mean and

unit variance. This removes the noise embedded in the fMRI recordings, and ensures that all the voxel time series, which are recorded from various subjects and sessions, are represented in the same scale.

- Interpolation methods are introduced since fMRI data does not have enough samples compared to the number of voxels in a brain volume. Interpolation step is the main focus of this study.

  - Sample generation by the polynomial interpolation method is introduced. A polynomial curve is fit to each voxel time series for a given puzzle. As a result, the newly generated voxel intensities are located in between the observed time instances. This method is used for sample generation after pre-processing.

  - A neural network is designed to increase temporal resolution as a second method. The voxel coordinate and the time form the input vector of the proposed neural network.

- Experiments are conducted to assess if a better brain decoding performance is achieved using the proposed method. After pre-processing, we end up with two data sets which consist of the selected voxel time series. SVM classification performances are reported on the data with the selected voxels.

  - First, the polynomial interpolation method is experimented with the different polynomial degrees. The generated data is used to train an SVM classifier. Then, the classifier is tested with the original fMRI data. 2% increase is observed compared to the pre-processed data sets.

  - Second, the neural network interpolation method is experimented on the pre-processed data sets. An SVM classifier is trained with the interpolated fMRI data and it is tested using the original fMRI data. About 3% increase is observed compared to the pre-processed data sets.

- The time series of a randomly selected voxel is plotted for the original and interpolated fMRI data. This is an important way of analyzing the nature of the data.

- The Fourier transform of the time series of a randomly selected voxel is plotted for the original and interpolated fMRI data. It shows that data generated with polynomial regression has a very similar frequency spectrum to the original data while the neural network interpolation introduces various frequencies. This is an important observation to be able to explain the results.

- Entropy analysis is conducted to compare the information content of the original and interpolated fMRI data. The entropies are calculated in anatomical region level. The entropy estimations for the lowest entropy regions are compared to justify the classification results.

5.2 Discussion

The proposed interpolation methods achieve a higher brain decoding performance compared to the original fMRI data. The baseline performance for the brain decoding is 85%. The polynomial interpolation method has a performance of 87% in brain decoding. It increases the performance around 2%, and this method is feasible in terms of run time and memory needs. On the other hand, we report that the suggested neural network method achieves a performance of 88% but this method takes a long time to complete. In addition to that, providing the memory and computational power required is impracticable. To get a notable performance increase, the neural network model is preferable but training the neural network is costly in terms of resources needed.

5.3 Future Work

The classical Multi-Layer Perceptron architecture, in our suggested neural network interpolation method, can be replaced by autoencoders and LSTM. Classifiers, other than SVM, can be used for evaluating the decoding performance.

REFERENCES

[1] A. Alchihabi, O. Ekmekci, B. B. Kivilcim, S. D. Newman, and F. T. Y. Vural. On the brain networks of complex problem solving. *arXiv preprint arXiv:1810.05077*, 2018.

[2] A. Alchihabi, B. B. Kivilicim, O. Ekmekci, S. D. Newman, and F. T. Y. Vural. Decoding cognitive subtasks of complex problem solving using fmri signals. In *2018 26th Signal Processing and Communications Applications Conference (SIU)*, pages 1–4. IEEE, 2018.

[3] A. Alchihabi, B. B. Kivilicim, S. D. Newman, and F. T. Y. Vural. A dynamic network representation of fmri for modeling and analyzing the problem solving task. In *2018 IEEE 15th International Symposium on Biomedical Imaging (ISBI 2018)*, pages 114–117, 2018.

[4] R. E. Bellman. *Adaptive control processes: a guided tour*, volume 2045. Princeton university press, 2015.

[5] D. D. Cox and R. Savoy. fmri brain reading: detecting and classifying distributed patterns of fmri activity in human visual cortex. *NeuroImage*, 19(2):261–270, 2003.

[6] R. C. Craddock, G. James, P. E. Holtzheimer III, X. P. Hu, and H. S. Mayberg. A whole brain fmri atlas generated via spatially constrained spectral clustering. *Human Brain Mapping*, 33(8):1914–1928, 2012.

[7] G. G. Değirmendereli and F. T. Yarman Vural. Representation of cognitive states by shannon entropy. In *2021 29th Signal Processing and Communications Applications Conference (SIU)*, pages 1–4, 2021.

[8] E. Formisano, F. D. Martino, and G. Valente. Multivariate analysis of fmri time

series: classification and regression of brain responses using machine learning. *Magnetic Resonance Imaging*, 26(7):921 – 934, 2008. Proceedings of the International School on Magnetic Resonance and Brain Function.

[9] G. H. Glover. Overview of functional magnetic resonance imaging. *Neurosurgery Clinics*, 22(2):133–139, 2011.

[10] G. Gunal Degirmendereli, S. D. Newman, and F. T. Yarman Vural. On the entropy of brain anatomic regions for complex problem solving. In *2019 IEEE 19th International Conference on Bioinformatics and Bioengineering (BIBE)*, pages 603–608, Oct 2019.

[11] C. Hughes, M.-H. Plumet, and M. Leboyer. Towards a cognitive phenotype for autism: Increased prevalence of executive dysfunction and superior spatial span amongst siblings of children with autism. *The Journal of Child Psychology and Psychiatry and Allied Disciplines*, 40(5):705–718, 1999.

[12] K. Katanoda, Y. Matsuda, and M. Sugishita. A spatio-temporal regression model for the analysis of functional mri data. *NeuroImage*, 17(3):1415–1428, 2002.

[13] B. B. Kivilcim, I. O. Ertugrul, and F. T. Yarman Vural. Modeling brain networks with artificial neural networks. In D. Stoyanov, Z. Taylor, E. Ferrante, A. V. Dalca, A. Martel, L. Maier-Hein, S. Parisot, A. Sotiras, B. Papiez, M. R. Sabuncu, and L. Shen, editors, *Graphs in Biomedical Image Analysis and Integrating Medical Imaging and Non-Imaging Modalities*, pages 43–53, Cham, 2018. Springer International Publishing.

[14] S. M. LaConte. Decoding fmri brain states in real-time. *Neuroimage*, 56(2):440–454, 2011.

[15] A. D. Lawrence, J. R. Hodges, A. E. Rosser, A. Kershaw, C. ffrench Constant, D. C. Rubinsztein, T. W. Robbins, and B. J. Sahakian. Evidence for specific cognitive deficits in preclinical Huntington's disease. *Brain*, 121(7):1329–1341, 07 1998.

[16] R. H. Lazeron, S. A. Rombouts, W. C. Machielsen, P. Scheltens, M. P. Witter, H. B. Uylings, and F. Barkhof. Visualizing brain activation during planning: The tower of london test adapted for functional mr imaging. *American Journal of Neuroradiology*, 21(8):1407–1414, 2000.

[17] R. G. Morris, J. J. Downes, B. J. Sahakian, J. L. Evenden, A. Heald, and T. W. Robbins. Planning and spatial working memory in parkinson's disease. *Journal of Neurology, Neurosurgery & Psychiatry*, 51(6):757–766, 1988.

[18] J. Mourão-Miranda, A. L. Bokde, C. Born, H. Hampel, and M. Stetter. Classifying brain states and determining the discriminating activation patterns: Support vector machine on functional mri data. *NeuroImage*, 28(4):980 – 995, 2005. Special Section: Social Cognitive Neuroscience.

[19] B. Mwangi, T. S. Tian, and J. C. Soares. A review of feature reduction techniques in neuroimaging. *Neuroinformatics*, 12(2):229–244, 2014.

[20] S. D. Newman, P. A. Carpenter, S. Varma, and M. A. Just. Frontal and parietal participation in problem solving in the tower of london: fmri and computational modeling of planning and high-level perception. *Neuropsychologia*, 41(12):1668 – 1682, 2003.

[21] S. D. Newman, J. A. Greco, and D. Lee. An fmri study of the tower of london: a look at problem structure differences. *Brain research*, 1286:123–132, 2009.

[22] S. D. Newman and G. Pittman. The tower of london: A study of the effect of problem structure on planning. *Journal of Clinical and Experimental Neuropsychology*, 29(3):333–342, 2007. PMID: 17454353.

[23] K. A. Norman, S. M. Polyn, G. J. Detre, and J. V. Haxby. Beyond mind-reading: multi-voxel pattern analysis of fmri data. *Trends in cognitive sciences*, 10(9):424–430, 2006.

[24] W. Olszowy, J. Aston, C. Rua, and G. B. Williams. Accurate autocorrelation modeling substantially improves fmri reliability. *Nature communications*, 10(1):1220, 2019.

[25] P. L. Purdon and R. M. Weisskoff. Effect of temporal autocorrelation due to physiological noise and stimulus paradigm on voxel-level false-positive rates in fmri. *Human brain mapping*, 6(4):239–249, 1998.

[26] A. Quirós, R. M. Diez, and D. Gamerman. Bayesian spatiotemporal model of fmri data. *NeuroImage*, 49(1):442–456, 2010.

[27] Rohith Gandhi. Support vector machine — introduction to machine learning algorithms, 2018. https://towardsdatascience.com/support-vector-machine-introduction-to-machine-learning-algorithms-934a444fca47.

[28] F. Rosenblatt. The perceptron: a probabilistic model for information storage and organization in the brain. *Psychological review*, 65(6):386, 1958.

[29] S. Ryali, K. Supekar, D. A. Abrams, and V. Menon. Sparse logistic regression for whole-brain classification of fmri data. *NeuroImage*, 51(2):752–764, 2010.

[30] M. L. Saxe GN, Calderone D. Brain entropy and human intelligence: A resting-state fmri study. *PLoS ONE 13(2): e0191582*, 2018.

[31] T. Shallice. Specific impairments of planning. *Philosophical transactions of the Royal Society of London. Series B, Biological sciences*, 298(1089):199—209, June 1982.

[32] C. E. Shannon. A mathematical theory of communication. *Bell System Technical Journal*, 27(3):379–423, 1948.

[33] Stephanie Watson. How fmri works, 2008. `https://science.howstuffworks.com/fmri.htm`, Last accessed on 2019-10-30.

[34] K. Uludag, D. J. Dubowitz, and R. B. Buxton. Basic principles of functional mri. *Clinical MRI. Elsevier, San Diego*, pages 249–287, 2005.

[35] V. N. Vapnik. An overview of statistical learning theory. *IEEE transactions on neural networks*, 10(5):988–999, 1999.

[36] Y. M. Wang, R. T. Schultz, R. T. Constable, and L. H. Staib. Nonlinear estimation and modeling of fmri data using spatio-temporal support vector re-

gression. In *Biennial International Conference on Information Processing in Medical Imaging*, pages 647–659. Springer, 2003.

[37] O. Yamashita, M.-a. Sato, T. Yoshioka, F. Tong, and Y. Kamitani. Sparse estimation automatically selects voxels relevant for the decoding of fmri activity patterns. *NeuroImage*, 42(4):1414–1429, 2008.

[38] P. Zhuang, A. G. Schwing, and O. Koyejo. Fmri data augmentation via synthesis. In *2019 IEEE 16th International Symposium on Biomedical Imaging (ISBI 2019)*, pages 1783–1787. IEEE, 2019.